The EMBO Journal (2004) 23, 212–220 | © 2004 European Molecular Biology Organization | All Rights Reserved 0261-4189/04
www.embojournal.org

THE EMBO JOURNAL

Akt negatively regulates the *in vitro* lifespan of human endothelial cells via a p53/p21-dependent pathway

Hideyuki Miyauchi[1], Tohru Minamino[1], Kaoru Tateno, Takeshige Kunieda, Haruhiro Toko and Issei Komuro*

Department of Cardiovascular Science and Medicine, Chiba University Graduate School of Medicine, Chuo-ku, Chiba, Japan

The signaling pathway of insulin/insulin-like growth factor-1/phosphatidylinositol-3 kinase/Akt is known to regulate longevity as well as resistance to oxidative stress in the nematode *Caenorhabditis elegans*. This regulatory process involves the activity of DAF-16, a forkhead transcription factor. Although reduction-of-function mutations in components of this pathway have been shown to extend the lifespan in organisms ranging from yeast to mice, activation of Akt has been reported to promote proliferation and survival of mammalian cells. Here we show that Akt activity increases along with cellular senescence and that inhibition of Akt extends the lifespan of primary cultured human endothelial cells. Constitutive activation of Akt promotes senescence-like arrest of cell growth via a p53/p21-dependent pathway, and inhibition of forkhead transcription factor FOXO3a by Akt is essential for this growth arrest to occur. FOXO3a influences p53 activity by regulating the level of reactive oxygen species. These findings reveal a novel role of Akt in regulating the cellular lifespan and suggest that the mechanism of longevity is conserved in primary cultured human cells and that Akt-induced senescence may be involved in vascular pathophysiology.

The EMBO Journal (2004) **23**, 212–220. doi:10.1038/sj.emboj.7600045; Published online 8 January 2004
Subject Categories: cell cycle; molecular biology of disease
Keywords: aging; Akt; endothelial cells; senescence

Introduction

Cellular senescence is the limited ability of primary human cells to divide when cultured *in vitro* and is accompanied by a specific set of changes in cell morphology, gene expression and function. These phenotypic changes have been implicated in human aging (Faragher and Kipling, 1998). This hypothesis, the cellular hypothesis of aging, was established by Hayflick (1975) and is supported by evidence that the replicative potential of primary cultured human cells is dependent on donor age and that the growth potential of cultured cells correlates well with the mean maximum lifespan of the species from which the cells are derived (Rohme, 1981), although some conflicting data have been reported (Cristofalo *et al*, 1998). Primary cultured cells obtained from patients with premature aging syndromes, such as Werner syndrome and Bloom syndrome, are known to have a shorter lifespan than the cells from age-matched healthy populations (Rohme, 1981; Thompson and Holliday, 1983), further supporting this hypothesis. Cell division is essential for the survival of multicellular organisms that contain renewable tissues, but also places the organism at the risk of developing cancer. It has been suggested that complex organisms have evolved at least two cellular mechanisms to prevent oncogenic transformation, which are apoptosis and cellular senescence (Campisi, 2001). Accordingly, age-associated diseases could be regarded as a by-product of the tumor suppressor mechanism, cellular senescence (Weinstein and Ciszek, 2002).

Many molecular mechanisms have been suggested to contribute to human aging and its associated diseases. Recent genetic analyses have demonstrated that reduction-of-function mutations in the signaling pathway of insulin/insulin-like growth factor-1 (IGF-1)/phosphatidylinositol-3 kinase (PI3K)/Akt (also known as protein kinase B) extend the longevity of the nematode *Caenorhabditis elegans* (Kenyon *et al*, 1993; Morris *et al*, 1996; Paradis and Ruvkun, 1998; Guarente and Kenyon, 2000; Kenyon, 2001; Lee *et al*, 2001; Lin *et al*, 2001; Longo and Finch, 2003). The forkhead transcription factor DAF-16, which is phosphorylated and thereby inactivated by Akt (Lee *et al*, 2001; Lin *et al*, 2001), plays an essential role in this longevity pathway (Lin *et al*, 1997; Ogg *et al*, 1997). More recently, it has been reported that the genes regulating longevity are conserved in organisms ranging from yeast to mice. Mutation of *Sch9*, which is homologous to *Akt*, extends the lifespan of yeast (Fabrizio *et al*, 2001), and mutations that decrease the activity of the insulin/IGF-1-like pathway increase the longevity of fruit flies (Tatar *et al*, 2001) and mice (Bluher *et al*, 2003; Holzenberger *et al*, 2003). These mutations that extend the lifespan are associated with increased resistance to oxidative stress, which is partly mediated by the increased expression of antioxidant genes (Honda and Honda, 1999; Fabrizio *et al*, 2003; Murphy *et al*, 2003).

In mammalian cells, activation of Akt has been reported to induce proliferation and survival, thereby promoting tumorigenesis (Datta *et al*, 1999; Blume-Jensen and Hunter, 2001; Testa and Bellacosa, 2001). Overexpression of Akt can transform NIH3T3 cells (Cheng *et al*, 1997), while introduction of Akt antisense RNA inhibits the tumorigenic phenotype of cancer cells expressing high levels of Akt (Cheng *et al*, 1996). The mechanisms by which Akt promotes cell proliferation and survival are likely to be multifactorial, because it has been reported to directly phosphorylate several components of the cell cycle machinery as well as the cell death machinery (Datta *et al*, 1999). Akt counteracts the effect of

*Corresponding author. Department of Cardiovascular Science and Medicine, Chiba University Graduate School of Medicine, 1-8-1 Inohana, Chuo-ku, Chiba 260-8670, Japan. Tel.: +81 43 226 2097; Fax: +81 43 226 2557; E-mail: komuro-tky@umin.ac.jp
[1]These authors contributed equally to this work

Received: 25 June 2003; accepted: 25 November 2003; Published online: 8 January 2004

cyclin-dependent kinase inhibitors on cell cycle progression by modulating their intracellular localization and level of transcription (Medema *et al*, 2000; Shin *et al*, 2002; Viglietto *et al*, 2002; Zhou *et al*, 2001a). Akt also increases the cyclin D1 level by inhibiting its degradation, which is important in the G1/S phase transition (Diehl *et al*, 1998). Moreover, it is known that Akt phosphorylates and inactivates proapoptotic factors such as BAD (Datta *et al*, 1997; del Peso *et al*, 1997) and procaspase-9 (Cardone *et al*, 1998), thereby promoting cell survival. Although these reports have suggested an important role of Akt in human malignancy (Blume-Jensen and Hunter, 2001; Testa and Bellacosa, 2001), it has mainly been examined in immortal cell lines and the impact of Akt activation on the growth and lifespan of primary cultured human cells is unknown.

In the present study, we found that inhibition of Akt could prolong the lifespan of primary cultured human endothelial cells, whereas constitutive activation of Akt promoted senescence-like growth arrest via a p53/p21-dependent pathway. Akt-induced growth arrest was inhibited by a mutated forkhead transcription factor that was resistant to Akt phosphorylation. These findings disclose a novel role of Akt in regulating the lifespan of cells and suggest that the mechanism of longevity is conserved in primary cultured human cells.

Results

Akt activation reduces the lifespan of human endothelial cells

We first investigated whether Akt activity was associated with cellular senescence of primary cultured human endothelial cells. Senescent endothelial cells had higher phospho-Akt levels than young endothelial cells (Figure 1A). To assess the actual role of Akt activity in regulating cellular lifespan, we infected primary cultured human endothelial cells with a retroviral vector encoding either constitutively activated myc-tagged Akt (AktCA) or dominant-negative myc-tagged Akt (AktDN). The empty retroviral vector pLNCX (Mock), encoding a neomycin resistance gene alone, was also transduced into endothelial cells as a control. Infected cells were purified using G418 for 7 days and then recultured until the cells underwent senescence. The 8th day after infection is designated as day 0 in all of the following experiments. Western blot analysis with anti-c-Myc antibody and anti-Akt antibody demonstrated that both AktCA and AktDN proteins were expressed by the endothelial cells, showing an approximately 4- to 8-fold increase of total Akt protein compared to endogenous Akt protein (Figure 1B). Long-term culture studies showed that constitutive activation of Akt significantly shortened the lifespan of the endothelial cells, whereas inhibition of Akt activity delayed senescence compared with mock-infected cells (Figure 1B). Introduction of AktDN influenced cellular lifespan in the late passages, but not in the early passages, suggesting that Akt activity increased with further cell division and thus promoted senescence. Expression of AktCA markedly reduced cell growth by day 7 (Figure 1C). AktCA-transduced endothelial cells were flattened and enlarged, while mock- or AktDN-infected endothelial cells exhibited normal morphology and growth (Figures 1C and D). Senescence-associated β-galactosidase activity was also increased in AktCA-transduced cells (Figure 1D). These changes of the phenotype, which were suggestive of senescence, were observed in various types of endothelial cells including microvascular endothelial cells (Supplementary Figure 1). The same senescence-like changes also occurred in confluent endothelial cells (Supplementary Figure 2). Thus, constitutive activation of Akt induced a senescence-like phenotype in human endothelial cells irrespective of the cell type and growth pattern. To further explore the relationship between Akt activity and cell growth, we isolated clones from AktCA-infected endothelial cells and determined the phospho-Akt level and the cell number on day 30. Clones obtained from mock-infected cell populations could be expanded up to $1\text{–}3 \times 10^6$ cells on average and revealed little Akt activity (Figure 1E, lane 1). In contrast, most of the AktCA-infected clones showed almost complete growth arrest and high levels of phospho-Akt expression (Figure 1E, lanes 5–7). However, some AktCA-infected clones showed low phospho-Akt levels and continued to proliferate (Figure 1E, lanes 2–4). Such proliferating populations may lead to underestimation of the growth inhibitory effect of AktCA in long-term culture experiments. The level of phospho-Akt was inversely correlated with the number of cells on day 30 (Figure 1E, right graph). Thus, we concluded that Akt is a negative regulator of the lifespan of primary cultured human endothelial cells.

Upregulation of p21 is essential for Akt-induced growth arrest

To clarify the mechanism of cell growth arrest induced by activation of Akt, we examined the expression of cell cycle regulatory proteins. Expression of p53 and $p21^{Waf1/Cip1}$, but not $p16^{Ink4a}$, was elevated, while the level of phosphorylated Rb was decreased in AktCA-infected cells compared with mock-infected cells (Figure 2A), suggesting that Akt may induce growth arrest by upregulating p53 and p21. To determine the role of p21 in Akt-induced cell growth arrest, we infected primary cultured mouse embryonic fibroblasts (MEF) derived from *p21*-deficient or wild-type mice with AktCA. Similar to endothelial cells, the growth of wild-type MEF was markedly reduced by activation of Akt compared with mock infection (Figure 2B, $p21^{+/+}$). In contrast, Akt-induced cell growth arrest was restored in *p21*-deficient MEF (Figure 2B, $p21^{-/-}$), suggesting that p21 is essential for Akt-induced growth arrest of these cells. It has been reported that expression of p21 is regulated by p53-dependent or -independent transcriptional mechanisms (el-Deiry *et al*, 1993) as well as protein degradation (Maki and Howley, 1997). To investigate the mechanism by which Akt activation increases p21 expression, we assessed the stability of p21 protein and the extent of *p21* transcription. The half-life of p21 protein did not differ between mock- and AktCA-infected endothelial cells (Figure 2C). Northern blot analysis revealed that the level of *p21* mRNA was significantly increased in Akt-infected cells compared with mock-infected cells (Figure 2D). Activation of Akt enhanced transcription of the luciferase reporter gene controlled by the promoter fragment of the human *p21* gene (Figure 2E), indicating that activation of Akt caused the transcriptional upregulation of p21 expression.

Critical role of p53 transcriptional activity in Akt-induced growth arrest

To ascertain whether Akt activation induces the transcriptional activity of p53, we transfected Akt-infected endothelial

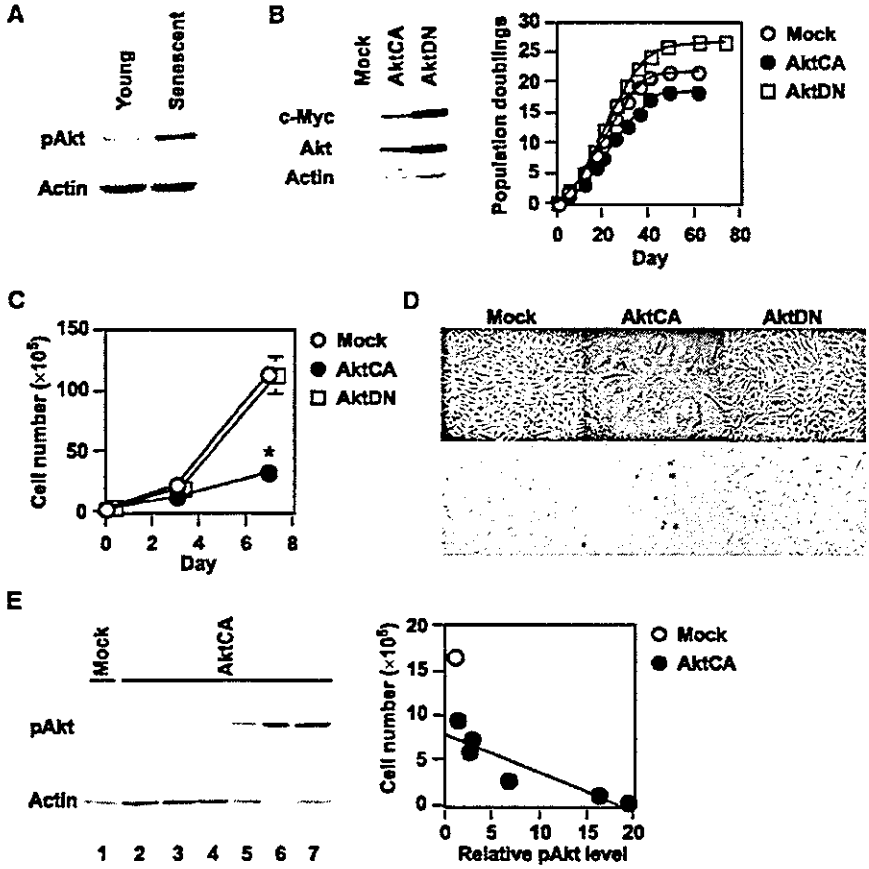

Figure 1 Akt negatively regulates the lifespan of primary cultured human endothelial cells. (**A**) Whole-cell lysates (30 μg) of young (passage 4) or senescent (passages 14–15) human endothelial cells were analyzed for the expression of phospho-Akt (pAkt, Ser473) and actin (loading control) by Western blotting. (**B**) Human endothelial cells were infected with pLNCX (Mock), AktCA or AktDN. After purification, infected cell populations were passaged until they underwent senescence, and the number of cumulative population doublings was determined. Similar results were obtained from three independent experiments. To validate the transduction of AktCA and AktDN, whole-cell lysates (30 μg) of each infected population were examined for the expression of exogenous myc-tagged Akt (c-Myc) and total Akt (Akt). (**C**) Human endothelial cells infected with pLNCX (Mock), AktCA or AktDN were purified with G418 for 7 days and seeded at a density of 3×10^5 cells per 100 mm plate on day 0. Cell number per 100 mm plate was then counted at indicated time points. $^*P<0.001$ versus Mock, ANOVA, $n=4$. (**D**) Cell morphology (upper panel) and senescence-associated β-galactosidase staining (lower panel) in endothelial cells infected with pLNCX (Mock), AktCA or AktDN. (**E**) Independent clones were isolated from pLNCX (Mock)- or AktCA-infected endothelial cells. At 30 days after isolation, the cell number of each clone was counted. Whole-cell lysates (~10 μg) of isolated clones were also prepared and analyzed for the expression of phospho-Akt by Western blotting (left panel, mock-infected clone for lane 1 and AktCA-infected clones for lanes 2–7). The cell number of each clone was as follows: 16.6×10^5 for lane 1; $6–10 \times 10^5$ for lanes 2–4; $0.1–2 \times 10^5$ for lanes 5–7. As the availability of samples was limited in the case of most AktCA-infected clones, the lysates used were less than 10 μg (lanes 5–7). Therefore, the levels of phospho-Akt were standardized on the basis of actin expression, and the relative level of phospho-Akt and the cell number of each clone were plotted in the graph (right panel, $r=0.92$, $P<0.01$). The corrected value of phospho-Akt in mock-infected clones (lane 1) is set at 1.

cells with the luciferase reporter gene containing 13 copies of the p53-binding consensus sequence (PG13). Introduction of AktCA induced *p53* promoter-driven luciferase activity compared with mock infection, but not luciferase activity driven by a promoter containing 15 copies of a similar sequence with mutation at critical positions (MG15) (Figure 3A). To further assess the relation between Akt and p53 transcription activity, we tested whether ablation of p53 could circumvent Akt-induced growth arrest. We infected human endothelial cells with a retroviral vector encoding the E6 oncoprotein of HPV16, which binds p53 and facilitates its destruction by ubiquitin-mediated proteolysis (pBabe E6). We also infected the same cells with the empty vector encoding resistance to puromycin alone (pBabe). Both cell populations were then subjected to infection with pLNCX or AktCA. Activation of Akt markedly inhibited the growth of pBabe-infected endothelial cells (Figure 3B, pBabe), while growth inhibition was completely abolished in E6-infected cells (Figure 3B, E6). Changes of cell morphology were also reversed to normal by introduction of E6 (Figure 3C). Ablation of p53 also lessened the decrease in the lifespan of AktCA-infected cells (Supplementary Figure 3). These results indicate a critical role of p53 in Akt-induced cell growth arrest. Introduction of AktCA did not induce p21 expression in E6-infected cells (Figure 3D), suggesting that constitutive activation of Akt increases induction of the transcription of *p21* by a p53-dependent mechanism and thereby promotes cell growth arrest.

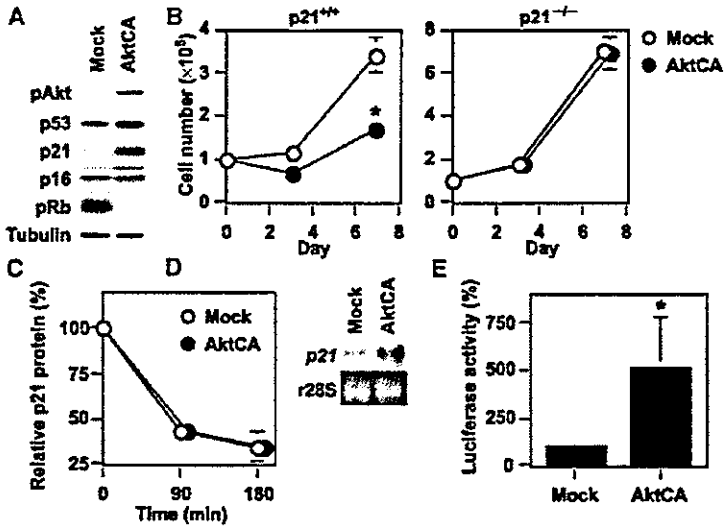

Figure 2 Upregulation of p21 is essential for Akt-induced growth arrest. (**A**) Whole-cell lysates (30 μg) of pLNCX (Mock)- or AktCA-infected endothelial cells on day 0 were examined for the expression of phospho-Akt (pAkt), cell cycle regulatory proteins and tubulin (loading control) by Western blotting. (**B**) MEF derived from wild-type ($p21^{-/-}$) or *p21*-deficient mice ($p21^{-/-}$) were infected with pLNCX (Mock) or AktCA, purified with G418 for 7 days and seeded at a density of 1×10^5 cells per 100 mm plate on day 0. Cell number per 100 mm plate was then counted at indicated time points. $^*P<0.001$ versus Mock, ANOVA, $n=4$. (**C**) Human endothelial cells infected with pLNCX (Mock) or AktCA were treated with cycloheximide (10 μg/ml) for the indicated time interval. Whole-cell lysates (30 μg) were then prepared at each time point and assayed for the expression of p21 and actin (loading control) by Western blotting. The graph indicates the results of densitometric analysis for the levels of p21 protein relative to actin expression. The value at time 0 is set at 100%. (**D**) Total RNA (30 μg) was extracted from human endothelial cells infected with pLNCX (Mock) or AktCA and analyzed for *p21* mRNA levels by Northern blotting (upper panel). Ribosomal RNA was used as an internal control (lower panel). (**E**) The luciferase reporter gene plasmid controlled by the promoter of the human *p21* gene was transfected into endothelial cells infected with pLNCX (Mock) or AktCA 24 h before the luciferase activity was measured. The activity in mock-infected cells is set at 100%. $^*P<0.05$ versus Mock, paired *t*-test, $n=4$.

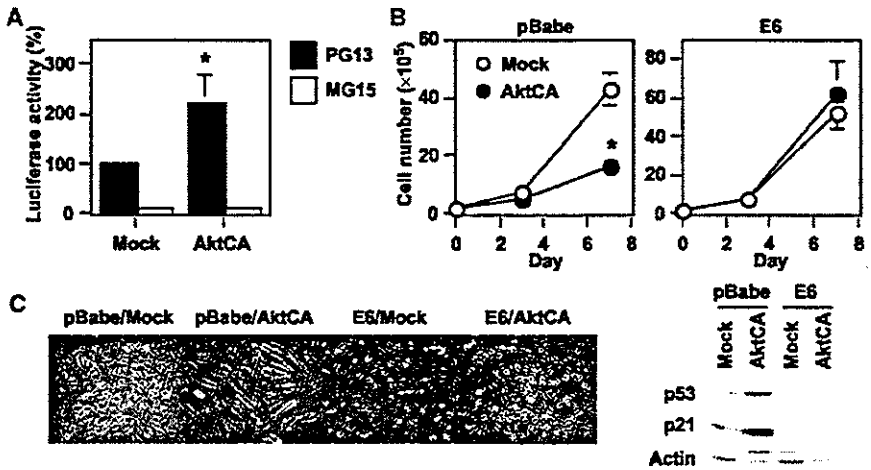

Figure 3 Critical role of p53 transcriptional activity in Akt-induced growth arrest. (**A**) The luciferase reporter gene plasmid pPG13-Luc containing the p53-binding sequence or pMG15-Luc containing the mutated p53-binding sequence was transfected into endothelial cells infected with pLNCX (Mock) or AktCA 24 h before the luciferase activity was measured. The activity of PG13-Luc in mock-infected cells is set at 100%. $^*P<0.005$ versus Mock, ANOVA, $n=4$. (**B**) Human endothelial cells were infected with pBabe (empty vector) or pBabe E6 and purified with puromycin. Infected cells were then transduced with pLNCX or AktCA as described in Figure 1C and seeded at a density of 2×10^5 cells per 100 mm plate on day 0. Cell number was then counted at indicated time points. $^*P<0.05$ versus Mock, ANOVA, $n=4$. (**C**) Morphology of cell populations prepared in (B). (**D**) Whole-cell lysates (30 μg) were extracted from cells prepared in (B) and examined for the expression of p53, p21 and actin (loading control).

Forkhead transcription factor mediates Akt-induced growth arrest

In *C. elegans*, a reduction-of-function mutation in the PI3K/Akt pathway leads to activation of the forkhead transcription factor DAF-16, resulting in extension of the lifespan, and this effect is inhibited by mutations of antioxidant genes (Murphy *et al*, 2003). Recent evidence indicates that the mammalian forkhead transcription factor FOXO3a (also known as FKHR-L1)

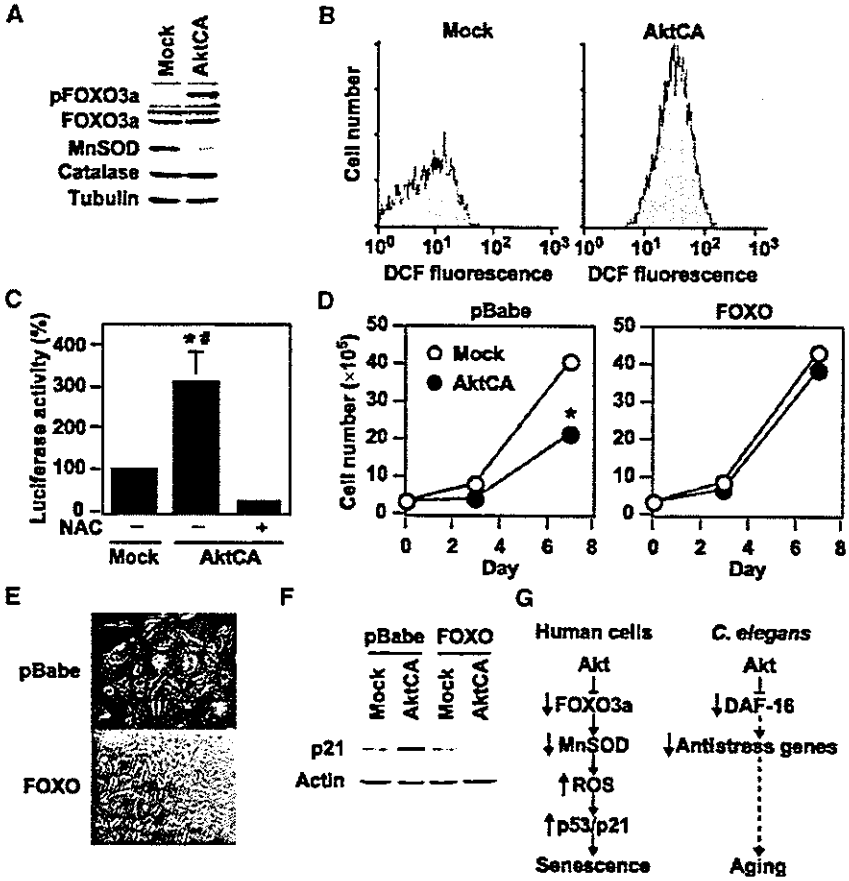

Figure 4 FOXO3a mediates Akt-induced growth arrest via the ROS/p53/p21-dependent mechanisms. (**A**) Whole-cell lysates (30 μg) of pLNCX (Mock)- or AktCA-infected endothelial cells were examined for expression of phospho-FOXO3a (pFOXO3a, Thr32), total FOXO3a (FOXO3a), MnSOD, catalase and tubulin (loading control) by Western blotting. (**B**) Human endothelial cells infected with pLNCX (Mock) or AktCA were loaded with DCF for 30 min and analyzed by FACS. Representative results from two independent experiments are shown. (**C**) The luciferase reporter gene plasmid PG13-Luc was transfected into endothelial cells infected with pLNCX (Mock) or AktCA and cultured in the absence or presence of NAC (0.5 mM). At 24 h after transfection, the luciferase activity was measured. The activity in mock-infected cells is set at 100%. $^{*}P<0.01$ versus Mock, $^{\#}P<0.001$ versus AktCA + NAC, ANOVA, $n=4$. (**D**) Human endothelial cells were infected with pBabe (empty vector) or pBabe mutant FOXO3a (FOXO). Infected cell populations were then transduced with pLNCX (Mock) or AktCA and seeded at a density of 3×10^5 cells per 100 mm plate on day 0. Cell number was then counted at indicated time points. $^{*}P<0.05$ versus Mock, ANOVA, $n=3$. (**E**) Morphology of Akt-infected cell populations prepared in (D). (**F**) Whole-cell lysates (30 μg) prepared in (D) were examined for the expression of p21 and actin (loading control) by Western blotting. Constitutive activation of Akt inhibits the transcriptional activity of FOXO3a and thereby downregulates *MnSOD*, leading to an increase of ROS that promotes senescence-like growth arrest via the p53/p21-dependent pathway. (**G**) Proposed signaling pathway of Akt-induced senescence in human endothelial cells compared with that in *C. elegans*. Akt inactivates FOXO3a and thereby downregulates its target antioxidant gene *MnSOD*, leading to an increase of ROS. ROS induces p53 activity, resulting in upregulation of p21 expression, which promotes cellular senescence in human endothelial cells. In *C. elegans*, the PI3K/Akt pathway also negatively regulates longevity by inactivating DAF-16 activity. This regulatory pathway partly involves the decreased expression of anti-stress genes including *SOD*.

upregulates radical scavenger genes that have a protective effect against oxidative damage in human cells (Kops *et al*, 2002; Nemoto and Finkel, 2002). To investigate the role of FOXO3a in Akt-induced growth arrest, we examined the expression of FOXO3a and antioxidant genes. Phosphorylated FOXO3a (the inactive form) was increased in AktCA-infected endothelial cells compared with mock-infected cells (Figure 4A). The level of manganese superoxide dismutase (MnSOD), but not catalase, was reduced in AktCA-infected endothelial cells (Figure 4A). Consistent with the decreased level of MnSOD, AktCA-infected endothelial cells exhibited an increase of reactive oxygen species (ROS), as assessed using the redox-sensitive fluorophore 2′,7′-dichlorofluorescein diacetate (DCF) (Figure 4B). Since oxidative stress is postulated to induce the activation of p53 (Finkel and Holbrook, 2000), we examined the effect of an ROS scavenger, *N*-acetyl cysteine (NAC), on *p53* promoter activity (PG13) in AktCA-infected endothelial cells. The enhancement of *p53* promoter-driven luciferase activity by AktCA was significantly lessened after treatment with NAC, suggesting that ROS are involved in Akt-induced senescence-like growth arrest (Figure 4C). To further determine the causal link between Akt-induced growth arrest and phosphorylation of FOXO3a, we tested a mutated FOXO3a that was resistant to phosphorylation by Akt. Introduction of this FOXO3a mutant prevented senescence-like growth arrest and cellular morphological changes induced by activation of

Akt (Figures 4D and E). Moreover, induction of p21 expression by Akt activation was effectively inhibited by the mutant form of FOXO3a (Figure 4F). These results suggest that constitutive activation of Akt inhibits the transcriptional activity of FOXO3a and thereby downregulates *MnSOD*, leading to an increase of ROS that promotes senescence-like growth arrest via the p53/p21-dependent pathway (Figure 4G). This signaling pathway could be recaptured in endothelial cells undergoing replicative senescence (Supplementary Figure 4), which suggests that Akt-induced growth arrest is relevant to physiological senescence and may also be involved in human vasculopathy.

Pathophysiological role of Akt-induced endothelial cell senescence

To investigate whether atherogenic stimuli could activate Akt in human atheroma tissues, we examined Akt activity in coronary arteries obtained at autopsy from patients who had ischemic heart disease. We detected Akt activity in endothelial cells on the surface of coronary atherosclerotic lesions, but not in those of the internal mammary arteries from the same patients, which showed minimal atherosclerotic changes (Figure 5A). To investigate the potential role of Akt-induced endothelial senescence in the pathogenesis of vasculopathy, we examined the effect of Akt on angiogenic activity and the expression of proinflammatory molecules. Tube formation by AktCA-infected endothelial cells was significantly reduced compared with that by mock-infected cells (Figure 5B). In addition, expression of intercellular adhesion molecule (ICAM)-1 was increased in AktCA-infected endothelial cells (Figure 5C). To further explore the role of Akt-induced senescence, we tested the influence of insulin on endothelial cell senescence. Treatment with insulin at a pathological dose caused increases in phospho-FOXO3a and p53 activity (Figures 6A and B), which were comparable to the changes seen in AktCA-infected cells. This increase was inhibited by introduction of AktDN (data not shown), indicating that it was dependent on Akt activity. Insulin induced p53 activity in a dose-dependent manner (Figure 6B). Moreover, continuous incubation with insulin was found to accelerate senescence of human endothelial cells, and this effect was also dose dependent (Figure 6C). Thus, it is conceivable that constitutive activation of Akt by growth factors may promote endothelial cell senescence and thereby contribute to vascular pathophysiology.

Discussion

Our results suggested a critical role of Akt activation in regulating the lifespan of primary cultured human cells in a manner similar to the control of longevity by the PI3K/Akt

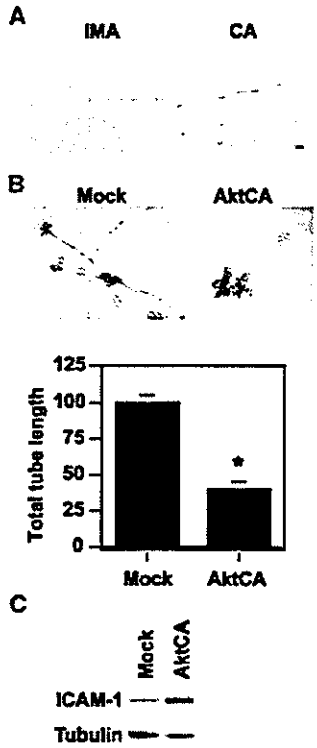

Figure 5 Pathophysiological role of Akt-induced endothelial cell senescence. (**A**) Immunohistochemistry for phospho-Akt (brown) in the coronary arteries (CA) and the internal mammary arteries (IMA) from the same patients. Scale bar: 10 μm. (**B**) Tube formation assay. Human endothelial cells infected with pLNCX (Mock) or AktCA were seeded onto Matrigel. After 48 h, the total tube length was estimated by an angiogenesis image analyzer (Kurabo, Osaka, Japan). The graph shows relative tube length in Mock- and AktCA-infected cells. The length in Mock-infected cells is set at 100%. $^{*}P<0.005$ versus Mock, unpaired *t*-test, $n=4$. (**C**) Whole-cell lysates (30 μg) of pLNCX (Mock)- or AktCA-infected endothelial cells were examined for the expression of ICAM-1 and tubulin (loading control) by Western blotting.

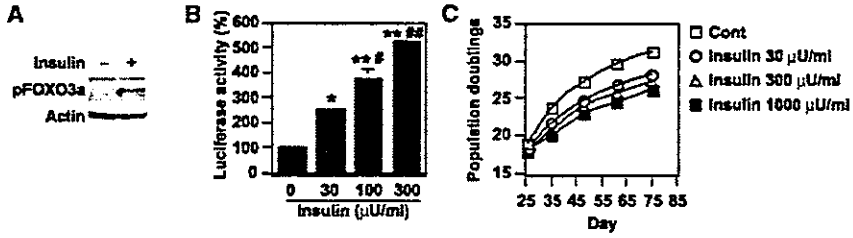

Figure 6 Insulin promotes endothelial cell senescence. (**A**) Whole-cell lysates (30 μg) of human endothelial cells treated with insulin (1000 μU/ml) for 30 min were analyzed for the levels of phosphorylated FOXO3a and actin (loading control) by Western blotting. (**B**) The luciferase reporter gene plasmid PG13-Luc was transfected into endothelial cells in the presence of insulin at the indicated dose. At 24 h after transfection, the luciferase activity was measured. The activity in controls is set at 100%. $^{*}P<0.05$, $^{**}P<0.0001$ versus control, $^{\#}P<0.01$, $^{\#\#}P<0.001$ versus insulin 30 μU/ml, $n=4$. (**C**) Human endothelial cells were cultured in the presence of insulin at the indicated dose and passaged. The number of cumulative population doublings was determined ($n=3$).

signaling pathway in *C. elegans*. We have previously demonstrated that senescent endothelial cells are present in human atherosclerotic plaques, but not nonatherosclerotic lesions, and express high levels of proinflammatory molecules that are known to promote atherogenesis (Minamino *et al*, 2002). Since Akt is known to be activated by various atherogenic stimuli (Cantley, 2002), our findings imply that constitutive activation of Akt by atherogenic stimuli may induce endothelial cell senescence in atheroma tissue and thereby contribute to atherogenesis. Consistent with this hypothesis, we observed that Akt was phosphorylated in human atheroma but not in normal arteries, and that expression of proinflammatory molecules was increased in AktCA-infected endothelial cells compared with mock-infected cells. Moreover, insulin increased p53 activity via an Akt-dependent mechanism and reduced the lifespan of endothelial cells. Thus, an Akt-induced senescence-like phenotype may be particularly involved in diabetic vasculopathy, since hyperinsulinemia could constitutively activate Akt in endothelial cells.

Although one supposes that Akt-induced senescence might be an artifact, the following points suggest that our findings are valid. First, we observed that Akt activity was increased in endothelial cells undergoing replicative senescence and that inhibition of this endogenous increase in Akt activity by AktDN led to prolongation of the cellular lifespan. This is compatible with many earlier studies demonstrating that reduction-of-function mutations in the insulin/PI3K/Akt pathway extend longevity in organisms ranging from yeast to mice (Longo and Finch, 2003). This signaling pathway (including phosphorylation of FOXO3a and downregulation of MnSOD induced by Akt) could be recaptured in endothelial cells undergoing replicative senescence (Supplementary Figure 4), which suggests that Akt-induced growth arrest may be relevant to physiological senescence. Second, we found that growth was significantly decreased in cloned populations obtained from cells infected with AktCA that exhibited a moderate increase in Akt activity (Figure 1, lanes 2–4). The level of Akt activity in these cells was similar to that in endothelial cells undergoing replicative senescence, suggesting that a physiological level of Akt activation may be able to promote cellular senescence. Third, we found that phospho-FOXO3a levels in AktCA-infected cells were comparable to those in endothelial cells stimulated by insulin at the level seen in patients with type II diabetes. The p53 transcriptional activity in AktCA-infected cells was also similar to that of cells treated with insulin. These results indicate that the pathophysiological activation of Akt was mimicked by infection with AktCA.

Gain-of-function mutations in the PI3K/Akt signaling pathway are frequently found in human cancers (Testa and Bellacosa, 2001). Thus, Akt-induced growth arrest may be another antitumorigenesis mechanism similar to Ras-induced senescence (Serrano *et al*, 1997; Campisi, 2001; Wright and Shay, 2001). We found that ablation of p53 prevented Akt-induced growth arrest, whereas both the p53- and p16-dependent pathways are reported to be essential for Ras-induced senescence (Serrano *et al*, 1997; Lin *et al*, 1998). Oncogenic Ras also induced premature senescence of primary cultured human vascular cells, which was suppressed by inhibition of mitogen-activated protein kinase kinase but not PI3K (Minamino *et al*, 2003), suggesting that Akt-induced growth arrest may be distinct from Ras-induced senescence. A recent study demonstrated that senescent cells could potentiate the oncogenic transformation of nearby normal cells (Krtolica *et al*, 2001), which suggests that induction of senescence by Akt as well as Ras may actually be pro-oncogenic.

We found that Akt increased the transcriptional activity of p53, resulting in upregulation of *p21* in primary cultured human endothelial cells. Our results are consistent with previous reports that Akt mediates induction of p21 expression by various stimuli in myoblasts and vascular cells (Lawlor and Rotwein, 2000a, b; Schonherr *et al*, 2001). However, Akt is also reported to induce cytoplasmic localization of p21 (Zhou *et al*, 2001a), thereby promoting cell proliferation, and to promote nuclear translocation of Mdm2 (a negative regulator of p53), leading to a reduction of both p53 levels and transactivation (Mayo and Donner, 2001; Zhou *et al*, 2001b). Such changes were not observed in human endothelial cells (H Miyauchi, unpublished data). It is noteworthy that most other studies have examined immortal cells, in which the normal cell cycle machinery might be impaired, and the effects of constitutive Akt activation have not been explored. Although the effects of tissue-specific transgenic expression of constitutively activated *Akt* alleles have been reported in several different murine models, most of these animals do not develop tumors (Vivanco and Sawyers, 2002), suggesting that activation of Akt is insufficient to cause cancer unless combined with other oncogenic stimuli. Thus, like Ras, Akt may promote cell proliferation and survival or senescence-like growth arrest, depending on various factors including the cellular context as well as the duration and extent of its activation.

In conclusion, we found that Akt negatively regulates the lifespan of primary cultured human endothelial cells via the p53/p21-dependent pathway, and this action is mediated at least partly by the forkhead transcription factor that regulates cellular ROS levels. Our data not only support the previous findings about the signaling pathway for longevity in *C. elegans*, but also provide a novel insight for research on the treatments of human vasculopathy and cancer.

Materials and methods

Cell culture

Human aortic endothelial cells, human dermal microvascular endothelial cells and human umbilical vein endothelial cells were purchased from Bio Whittaker (Walkersville, MD), and cultured according to the manufacturer's instructions. These cells gave similar results (data not shown). We defined senescent cells as the cultures that do not increase in the cell number and remain subconfluent for 2 weeks. We confirmed the senescent phenotype with SA-β-gal activity assay. Wild-type and *p21*-deficient MEFs were prepared from day 13.5 embryos derived from crosses between $p21^{+/-}$ mice (Jackson, Bar Harbor, ME) and cultured in DMEM plus 10% fetal bovine serum. Senescence-associated β-galactosidase staining was performed as described (Minamino *et al*, 2002). Tube formation assay was performed according to the manufacturer's instructions (BioCoat Angiogenesis System, Clontech, Palo Alto, CA).

Retroviral infection

The following plasmids were used for generating retroviruses: pLNCX (Clontech, Palo Alto, CA) and pBabe (a gift from Dr CW Lowe, Cold Spring Harbor Laboratory, Cold Spring Harbor, NY). We created the pLNCX-based vector expressing a constitutively active form of Akt (AktCA) or a dominant-negative form of Akt (AktDN) by using the fragment derived from the plasmid pBS-CA-Akt or

pBS-DN-Akt (Fujishiro *et al*, 2001), respectively (a gift from Dr T Asano, Tokyo University, Tokyo, Japan). The pBabe-based vector expressing a mutant form of FOXO3a was constructed by using the fragment derived from pECE FOXO3aTM (Brunet *et al*, 1999) (a gift from Dr ME Greenberg, Harvard Medical School, Boston, MA). We also constructed the pBabe-based vector expressing E6 (pBabe E6). Details of the construct are available upon request. Retroviral stocks were generated by transient transfection of packaging cell line (PT67, Clontech) and stored at −80°C until use. Human endothelial cells (passage 4–6) were plated at 5×10^5 cells per 100-mm-diameter dish 24 h before infections. For infections, the culture medium was replaced by retroviral stocks supplemented with 8 μg/ml polybrene (Sigma, Tokyo, Japan). At 48 h after infections, the infected cell populations were selected by culture in 500 μg/ml G418 for 7 days (pLNCX-based vectors). After selection, $1–3 \times 10^5$ cells were seeded onto 100-mm-diameter dishes on the 8th day postinfection. The 8th day after infection is designated as day 0. For double infection, endothelial cells were infected with pBabe, pBabe FOXO3a or pBabe E6 purified with 0.8 μg/ml puromycin for 4 days and subjected to the second infection as described above.

Western blotting and antibodies

Whole-cell lysates (30 μg) were resolved by SDS polyacrylamide gel electrophoresis (PAGE). Proteins were transferred onto a polyvinylidene difluoride (PVDF) membrane (Millipore, Bedford, MA) and incubated with the first antibody followed by an anti-rabbit immunoglobulin G–horseradish peroxidase antibody or anti-mouse immunoglobulin G–horseradish peroxidase antibody (Jackson, West Grove, PA). Specific proteins were detected using enhanced chemiluminescence (Amersham, Tokyo, Japan). The first antibodies used for Western blotting are as follows: antibodies to Akt, p53, ICAM-1, actin and tubulin (Santa Cruz, Santa Cruz, CA); antibodies to retinoblastoma protein and p16 (Pharmingen, Tokyo, Japan); anti-p21 antibody (Oncogene, Cambridge, MA); anti-phospho-Akt (Ser473) antibody (Cell Signaling, Beverly, MA); anti-catalase antibody (Sigma); antibodies to FOXO3a, phospho-FOXO3a (Thr32) and MnSOD (Upstate Biotechnology, Lake Placid, NY).

Northern blotting

Total RNA (30 μg) was extracted using RNA zol B (Tel Test, Friendswood, TX) according to the manufacturer's instructions, separated on a formaldehyde denaturing gel and transferred to a nylon membrane (Amersham). The blot was then hybridized with radiolabeled p21 cDNA probes using the Quickhyb hybridization solution (Stratagene, Tokyo, Japan) according to the manufacturer's instructions.

Luciferase assays

The reporter gene plasmid (1 μg) was transfected into endothelial cells infected with pLNCX (Mock) or AktCA 24 h before luciferase assay. The control vector encoding *Renilla* luciferase (0.1 μg) was co-transfected for an internal control. Luciferase assay was carried out using a dual-luciferase reporter assay system (Promega, Madison, WI) according to the manufacturer's instructions. The plasmids pPG13-Luc, pPG15-Luc and pWWP-LUC-1 (el-Deiry *et al*, 1993) were a gift from Dr B Vogelstein (Johns Hopkins University, Baltimore, MD).

Tissue specimens and histology

Human coronary arteries and internal mammary arteries were obtained from four autopsied individuals who had ischemic heart disease. For immunohistochemistry, the frozen sections (6 μm) were treated with 0.3% hydrogen peroxide in methanol for 20 min, preincubated with 5% goat serum and then treated with anti-phospho-Akt antibody (1:100; Santa Cruz, Santa Cruz, CA) for 1 h at 37°C. Next, the sections were incubated with a biotinylated goat secondary antibody, treated with the avidin–biotin complex (Elite ABC kit, Vector, Burlingame, CA) and stained with diaminobenzidine tetrahydrochloride and hydrogen peroxide. To verify the specificity of the first antibodies, we performed a control staining with nonimmune IgG and excluded the possibility of nonspecific signals. The studies on human samples were approved by our institutional review board.

Statistical analysis

All values were expressed as mean±s.e.m. Comparison of results between different groups was performed by one-way analysis of variance, paired *t*-test and unpaired *t*-test using StatView 4.5 (Abacus Concepts, Berkeley, CA).

Supplementary data

Supplementary data are available at *The EMBO Journal* Online.

Acknowledgements

We thank Dr B Vogelstein, SW Lowe, ME Greenberg and T Asano for reagents. This work was supported by grants from Takeda Medical Research Foundation, Takeda Science Foundation, Japan Heart Foundation, Mochida Memorial Foundation, Uehara Memorial Foundation, Mitsubishi Pharma Research Foundation and the Ministry of Education, Science, Sports, and Culture of Japan (to TM and IK).

Competing interests statement

The authors declare that they have no competing financial interests.

References

Bluher M, Kahn BB, Kahn CR (2003) Extended longevity in mice lacking the insulin receptor in adipose tissue. *Science* **299**: 572–574

Blume-Jensen P, Hunter T (2001) Oncogenic kinase signalling. *Nature* **411**: 355–365

Brunet A, Bonni A, Zigmond MJ, Lin MZ, Juo P, Hu LS, Anderson MJ, Arden KC, Blenis J, Greenberg ME (1999) Akt promotes cell survival by phosphorylating and inhibiting a Forkhead transcription factor. *Cell* **96**: 857–868

Campisi J (2001) Cellular senescence as a tumor-suppressor mechanism. *Trends Cell Biol* **11**: S27–S31

Cantley LC (2002) The phosphoinositide 3-kinase pathway. *Science* **296**: 1655–1657

Cardone MH, Roy N, Stennicke HR, Salvesen GS, Franke TF, Stanbridge E, Frisch S, Reed JC (1998) Regulation of cell death protease caspase-9 by phosphorylation. *Science* **282**: 1318–1321

Cheng JQ, Altomare DA, Klein MA, Lee WC, Kruh GD, Lissy NA, Testa JR (1997) Transforming activity and mitosis-related expression of the AKT2 oncogene: evidence suggesting a link between cell cycle regulation and oncogenesis. *Oncogene* **14**: 2793–2801

Cheng JQ, Ruggeri B, Klein WM, Sonoda G, Altomare DA, Watson DK, Testa JR (1996) Amplification of AKT2 in human pancreatic cells and inhibition of AKT2 expression and tumorigenicity by antisense RNA. *Proc Natl Acad Sci USA* **93**: 3636–3641

Cristofalo VJ, Allen RG, Pignolo RJ, Martin BG, Beck JC (1998) Relationship between donor age and the replicative lifespan of human cells in culture: a reevaluation. *Proc Natl Acad Sci USA* **95**: 10614–10619

Datta SR, Brunet A, Greenberg ME (1999) Cellular survival: a play in three Akts. *Genes Dev* **13**: 2905–2927

Datta SR, Dudek H, Tao X, Masters S, Fu H, Gotoh Y, Greenberg ME (1997) Akt phosphorylation of BAD couples survival signals to the cell-intrinsic death machinery. *Cell* **91**: 231–241

del Peso L, Gonzalez-Garcia M, Page C, Herrera R, Nunez G (1997) Interleukin-3-induced phosphorylation of BAD through the protein kinase Akt. *Science* **278**: 687–689

Diehl JA, Cheng M, Roussel MF, Sherr CJ (1998) Glycogen synthase kinase-3beta regulates cyclin D1 proteolysis and subcellular localization. *Genes Dev* **12**: 3499–3511

el-Deiry WS, Tokino T, Velculescu VE, Levy DB, Parsons R, Trent JM, Lin D, Mercer WE, Kinzler KW, Vogelstein B (1993) WAF1, a potential mediator of p53 tumor suppression. *Cell* **75**: 817–825

Fabrizio P, Liou LL, Moy VN, Diaspro A, SelverstoneValentine J, Gralla EB, Longo VD (2003) SOD2 functions downstream of Sch9 to extend longevity in yeast. *Genetics* **163**: 35–46

Fabrizio P, Pozza F, Pletcher SD, Gendron CM, Longo VD (2001) Regulation of longevity and stress resistance by Sch9 in yeast. *Science* **292**: 288–290

Faragher RG, Kipling D (1998) How might replicative senescence contribute to human ageing? *BioEssays* **20:** 985–991
Finkel T, Holbrook NJ (2000) Oxidants, oxidative stress and the biology of ageing. *Nature* **408:** 239–247
Fujishiro M, Gotoh Y, Katagiri H, Sakoda H, Ogihara T, Anai M, Onishi Y, Ono H, Funaki M, Inukai K, Fukushima Y, Kikuchi M, Oka Y, Asano T (2001) MKK6/3 and p38 MAPK pathway activation is not necessary for insulin-induced glucose uptake but regulates glucose transporter expression. *J Biol Chem* **276:** 19800–19806
Guarente L, Kenyon C (2000) Genetic pathways that regulate ageing in model organisms. *Nature* **408:** 255–262
Hayflick L (1975) Current theories of biological aging. *Fed Proc* **34:** 9–13
Holzenberger M, Dupont J, Ducos B, Leneuve P, Geloen A, Even PC, Cervera P, Le Bouc Y (2003) IGF-1 receptor regulates lifespan and resistance to oxidative stress in mice. *Nature* **421:** 182–187
Honda Y, Honda S (1999) The daf-2 gene network for longevity regulates oxidative stress resistance and Mn-superoxide dismutase gene expression in *Caenorhabditis elegans*. *FASEB J* **13:** 1385–1393
Kenyon C (2001) A conserved regulatory system for aging. *Cell* **105:** 165–168
Kenyon C, Chang J, Gensch E, Rudner A, Tabtiang R (1993) A *C. elegans* mutant that lives twice as long as wild type. *Nature* **366:** 461–464
Kops GJ, Dansen TB, Polderman PE, Saarloos I, Wirtz KW, Coffer PJ, Huang TT, Bos JL, Medema RH, Burgering BM (2002) Forkhead transcription factor FOXO3a protects quiescent cells from oxidative stress. *Nature* **419:** 316–321
Krtolica A, Parrinello S, Lockett S, Desprez PY, Campisi J (2001) Senescent fibroblasts promote epithelial cell growth and tumorigenesis: a link between cancer and aging. *Proc Natl Acad Sci USA* **98:** 12072–12077
Lawlor MA, Rotwein P (2000a) Coordinate control of muscle cell survival by distinct insulin-like growth factor activated signaling pathways. *J Cell Biol* **151:** 1131–1140
Lawlor MA, Rotwein P (2000b) Insulin-like growth factor-mediated muscle cell survival: central roles for Akt and cyclin-dependent kinase inhibitor p21. *Mol Cell Biol* **20:** 8983–8995
Lee RY, Hench J, Ruvkun G (2001) Regulation of *C. elegans* DAF-16 and its human ortholog FKHRL1 by the daf-2 insulin-like signaling pathway. *Curr Biol* **11:** 1950–1957
Lin AW, Barradas M, Stone JC, van Aelst L, Serrano M, Lowe SW (1998) Premature senescence involving p53 and p16 is activated in response to constitutive MEK/MAPK mitogenic signaling. *Genes Dev* **12:** 3008–3019
Lin K, Dorman JB, Rodan A, Kenyon C (1997) daf-16: An HNF-3/forkhead family member that can function to double the life-span of *Caenorhabditis elegans*. *Science* **278:** 1319–1322
Lin K, Hsin H, Libina N, Kenyon C (2001) Regulation of the *Caenorhabditis elegans* longevity protein DAF-16 by insulin/IGF-1 and germline signaling. *Nat Genet* **28:** 139–145
Longo VD, Finch CE (2003) Evolutionary medicine: from dwarf model systems to healthy centenarians? *Science* **299:** 1342–1346
Maki CG, Howley PM (1997) Ubiquitination of p53 and p21 is differentially affected by ionizing and UV radiation. *Mol Cell Biol* **17:** 355–363
Mayo LD, Donner DB (2001) A phosphatidylinositol 3-kinase/Akt pathway promotes translocation of Mdm2 from the cytoplasm to the nucleus. *Proc Natl Acad Sci USA* **98:** 11598–11603
Medema RH, Kops GJ, Bos JL, Burgering BM (2000) AFX-like Forkhead transcription factors mediate cell-cycle regulation by Ras and PKB through p27kip1. *Nature* **404:** 782–787
Minamino T, Miyauchi H, Yoshida T, Ishida Y, Yoshida H, Komuro I (2002) Endothelial cell senescence in human atherosclerosis: role of telomere in endothelial dysfunction. *Circulation* **105:** 1541–1544
Minamino T, Yoshida T, Tateno K, Miyauchi H, Zou Y, Toko H, Komuro I (2003) Ras-induced vascular smooth muscle cell senescence in human atherosclerosis. *Circulation* **108:** 2264–2269
Morris JZ, Tissenbaum HA, Ruvkun G (1996) A phosphatidylinositol-3-OH kinase family member regulating longevity and diapause in *Caenorhabditis elegans*. *Nature* **382:** 536–539
Murphy CT, McCarroll SA, Bargmann CI, Fraser A, Kamath RS, Ahringer J, Li H, Kenyon C (2003) Genes that act downstream of DAF-16 to influence the lifespan of *Caenorhabditis elegans*. *Nature* **424:** 277–283
Nemoto S, Finkel T (2002) Redox regulation of forkhead proteins through a p66shc-dependent signaling pathway. *Science* **295:** 2450–2452
Ogg S, Paradis S, Gottlieb S, Patterson GI, Lee L, Tissenbaum HA, Ruvkun G (1997) The Fork head transcription factor DAF-16 transduces insulin-like metabolic and longevity signals in *C. elegans*. *Nature* **389:** 994–999
Paradis S, Ruvkun G (1998) *Caenorhabditis elegans* Akt/PKB transduces insulin receptor-like signals from AGE-1 PI3 kinase to the DAF-16 transcription factor. *Genes Dev* **12:** 2488–2498
Rohme D (1981) Evidence for a relationship between longevity of mammalian species and life spans of normal fibroblasts *in vitro* and erythrocytes *in vivo*. *Proc Natl Acad Sci USA* **78:** 5009–5013
Schonherr E, Levkau B, Schaefer L, Kresse H, Walsh K (2001) Decorin-mediated signal transduction in endothelial cells. Involvement of Akt/protein kinase B in up-regulation of p21(WAF1/CIP1) but not p27(KIP1). *J Biol Chem* **276:** 40687–40692
Serrano M, Lin AW, McCurrach ME, Beach D, Lowe SW (1997) Oncogenic ras provokes premature cell senescence associated with accumulation of p53 and p16INK4a. *Cell* **88:** 593–602
Shin I, Yakes FM, Rojo F, Shin NY, Bakin AV, Baselga J, Arteaga CL (2002) PKB/Akt mediates cell-cycle progression by phosphorylation of p27(Kip1) at threonine 157 and modulation of its cellular localization. *Nat Med* **8:** 1145–1152
Tatar M, Kopelman A, Epstein D, Tu MP, Yin CM, Garofalo RS (2001) A mutant *Drosophila* insulin receptor homolog that extends life-span and impairs neuroendocrine function. *Science* **292:** 107–110
Testa JR, Bellacosa A (2001) AKT plays a central role in tumorigenesis. *Proc Natl Acad Sci USA* **98:** 10983–10985
Thompson KV, Holliday R (1983) Genetic effects on the longevity of cultured human fibroblasts. II. DNA repair deficient syndromes. *Gerontology* **29:** 83–88
Viglietto G, Motti ML, Bruni P, Melillo RM, D'Alessio A, Califano D, Vinci F, Chiappetta G, Tsichlis P, Bellacosa A, Fusco A, Santoro M (2002) Cytoplasmic relocalization and inhibition of the cyclin-dependent kinase inhibitor p27(Kip1) by PKB/Akt-mediated phosphorylation in breast cancer. *Nat Med* **8:** 1136–1144
Vivanco I, Sawyers CL (2002) The phosphatidylinositol 3-Kinase AKT pathway in human cancer. *Nat Rev Cancer* **2:** 489–501
Weinstein BS, Ciszek D (2002) The reserve-capacity hypothesis: evolutionary origins and modern implications of the trade-off between tumor-suppression and tissue-repair. *Exp Gerontol* **37:** 615–627
Wright WE, Shay JW (2001) Cellular senescence as a tumor-protection mechanism: the essential role of counting. *Curr Opin Genet Dev* **11:** 98–103
Zhou BP, Liao Y, Xia W, Spohn B, Lee MH, Hung MC (2001a) Cytoplasmic localization of p21Cip1/WAF1 by Akt-induced phosphorylation in HER-2/neu-overexpressing cells. *Nat Cell Biol* **3:** 245–252
Zhou BP, Liao Y, Xia W, Zou Y, Spohn B, Hung MC (2001b) HER-2/neu induces p53 ubiquitination via Akt-mediated MDM2 phosphorylation. *Nat Cell Biol* **3:** 973–982

nature medicine

ARTICLES

Salt-sensitive hypertension is triggered by Ca^{2+} entry via Na^+/Ca^{2+} exchanger type-1 in vascular smooth muscle

Takahiro Iwamoto[1,3], Satomi Kita[1,5], Jin Zhang[2], Mordecai P Blaustein[2], Yuji Arai[4], Shigeru Yoshida[5], Koji Wakimoto[6], Issei Komuro[7] & Takeshi Katsuragi[1]

Excessive salt intake is a major risk factor for hypertension. Here we identify the role of Na^+/Ca^{2+} exchanger type 1 (NCX1) in salt-sensitive hypertension using SEA0400, a specific inhibitor of Ca^{2+} entry through NCX1, and genetically engineered mice. SEA0400 lowers arterial blood pressure in salt-dependent hypertensive rat models, but not in other types of hypertensive rats or in normotensive rats. Infusion of SEA0400 into the femoral artery in salt-dependent hypertensive rats increases arterial blood flow, indicating peripheral vasodilation. SEA0400 reverses ouabain-induced cytosolic Ca^{2+} elevation and vasoconstriction in arteries. Furthermore, heterozygous NCX1-deficient mice have low salt sensitivity, whereas transgenic mice that specifically express NCX1.3 in smooth muscle are hypersensitive to salt. SEA0400 lowers the blood pressure in salt-dependent hypertensive mice expressing NCX1.3, but not in SEA0400-insensitive NCX1.3 mutants. These findings indicate that salt-sensitive hypertension is triggered by Ca^{2+} entry through NCX1 in arterial smooth muscle and suggest that NCX1 inhibitors might be useful therapeutically.

Hypertension is the most common chronic disease, and is the leading risk factor for death that is due to stroke, myocardial infarction or end-stage renal failure[1,2]. The critical importance of excess salt intake in the pathogenesis of hypertension is widely recognized[3–6], but the mechanism by which excess salt intake elevates blood pressure has puzzled researchers. Recently discovered cardiotonic steroids (CTS), such as endogenous ouabain[7], and other steroids[8–10], including marinobufagenin, proscillaridin A and bufalin, have been proposed as candidate intermediaries. In humans, a chronic high-salt diet causes a rise in plasma CTS[11–13]. Moreover, ~50% of patients with essential hypertension have substantially elevated levels of endogenous ouabain[14,15]. Plasma CTS are also high in several salt-dependent hypertensive animals[7,13,16]. Indeed, PST2238, a ouabain antagonist, lowers blood pressure in salt-dependent hypertensive rats and in certain patients with essential hypertension[17,18]. Generally, it is believed that CTS inhibit the plasma membrane Na^+/K^+ ATPase, the 'sodium-potassium pump,' and lead to an increase in cytosolic Na^+ concentration ($[Na^+]_{cyt}$). Cellular Na^+ accumulation raises the cytosolic Ca^{2+} concentration ($[Ca^{2+}]_{cyt}$) through the involvement of the Na^+/Ca^{2+} exchanger (NCX), and thereby increases contraction in vascular or heart muscle. This may lead to hypertension[19], but the hypothesis has not yet been critically tested because little is understood of the function of NCX in these processes.

NCX is a plasma membrane transporter expressed in various cell types. Membrane potential and transmembrane gradients of Na^+ and Ca^{2+} control this bidirectional exchanger. The mammalian NCX family comprises three isoforms[20]. NCX1 is abundant in the heart, but is also expressed in many other tissues. In contrast, expression of NCX2 and NCX3 is restricted to brain and skeletal muscle. Extensive alternative splicing of NCX1 generates tissue-specific variants[21–23]; the heart expresses exclusively NCX1.1, and vascular tissue predominantly NCX1.3 and NCX1.7. Although the importance of this diversity is unclear, it may reflect different requirements for the maintenance of Ca^{2+} homeostasis in various cell types[20]. In cardiomyocytes, NCX1 has the primary role in Ca^{2+} extrusion during excitation-contraction coupling[24]. Under pathological conditions such as cardiac ischemia-reperfusion injury[25,26], NCX1 is thought to cause Ca^{2+} overload resulting from elevated $[Na^+]_{cyt}$; this leads to cardiac dysfunction. In other tissues, including vascular smooth muscle (VSM), NCX1 is also believed to extrude Ca^{2+} from the cytosol[25], but the physiological roles of vascular NCX1 are still unclear.

Recently, SEA0400, a specific NCX inhibitor that preferentially blocks the Ca^{2+} entry mode[27,28], was developed. We now report that SEA0400 lowers arterial blood pressure in salt- or ouabain-dependent hypertensive models, but not in normotensive rats or in other types of hypertensive rats. SEA0400 reverses the cytosolic Ca^{2+} elevation and vasoconstriction induced by nanomolar ouabain. Furthermore, we found that heterozygous mice with reduced expression of NCX1 resist development of salt-dependent hypertension. Conversely, transgenic mice with VSM-specific expression of NCX1 readily develop hypertension after high salt intake. These data provide compelling

[1]Department of Pharmacology, School of Medicine, Fukuoka University, Fukuoka 814-0180, Japan. [2]Department of Physiology, University of Maryland School of Medicine, Baltimore, Maryland 21201, USA. Departments of [3]Molecular Physiology and [4]Bioscience, National Cardiovascular Center Research Institute, Osaka 565-8565, Japan. [5]Medicinal Research Laboratories, Taisho Pharmaceutical Co., Ltd., Saitama 330-8530, Japan. [6]Discovery Research Laboratory, Tanabe Seiyaku Co., Ltd., Osaka 532-8505, Japan. [7]Department of Cardiovascular Science and Medicine, Chiba University Graduate School of Medicine, Chiba 260-8670, Japan. Correspondence should be addressed to T.I. (tiwamoto@cis.fukuoka-u.ac.jp).

Published online 10 October 2004; doi:10.1038/nm1118

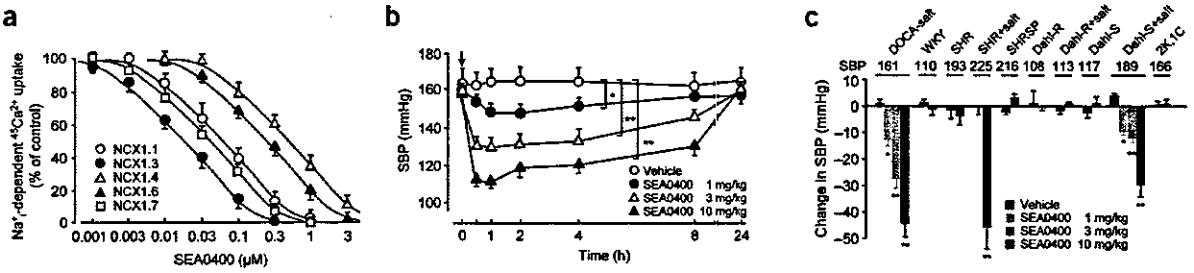

Figure 1 NCX1 inhibition and antihypertensive effects of SEA0400. (**a**) Concentration-response curves of SEA0400 for intracellular Na^+ (Na^+_i)-dependent $^{45}Ca^{2+}$ uptake into fibroblasts overexpressing variously spliced isoforms of human NCX1. Expression levels and NCX activities in these transfectants are shown in **Supplementary Figure 1** online. (**b**) Recordings over 24 h (9 a.m. to 9 a.m.) of SBP after oral administration of vehicle or SEA0400 (1–10 mg/kg) in DOCA-salt hypertensive rats. (**c**) Peak changes in SBP in various types of hypertensive rats treated with oral SEA0400. SHR, Dahl salt-resistant rats (Dahl-R) and Dahl salt-sensitive rats (Dahl-S) were fed a normal (0.3% NaCl) or high-salt diet (8% NaCl; +salt) for 4–6 weeks. Change in SBP in mmHg for the respective rats is indicated. Bars represent means ± s.e.m. ($n = 4$–6). WKY, Wistar Kyoto rats; SHRSP, stroke-prone SHR; 2K,1C, two-kidney, one-clip rats. $^*P < 0.05$, $^{**}P < 0.01$ compared with each vehicle group.

evidence that salt-dependent hypertension is triggered by Ca^{2+} entry through NCX1 in VSM cells. This finding also suggests that vascular NCX1 is a new therapeutic or diagnostic target for salt-sensitive hypertension.

RESULTS

Antihypertensive effects of SEA0400

In VSM cells, NCX1.3 and NCX1.7 are the dominant splicing isoforms[21–23]. By measuring intracellular Na^+-dependent Ca^{2+} uptake into fibroblasts overexpressing splicing isoforms of NCX1, we found that SEA0400, a specific inhibitor for Ca^{2+} entry through NCX1, preferentially blocks the vascular isoforms, especially NCX1.3 (**Fig. 1a** and **Supplementary Fig. 1** online). This finding indicates that SEA0400 is an excellent pharmacological tool for studying the vascular function of NCX1.

To evaluate the role of NCX1 in hypertension, we tested the effects of SEA0400 on various hypertensive models. A single oral dose of SEA0400 (1–10 mg/kg) caused a dose-dependent and long-lasting decrease in systolic blood pressure (SBP) in deoxycorticosterone acetate (DOCA)-salt hypertensive rats (Fig. 1b). Intravenous administration of SEA0400 (0.3–3 mg/kg) also lowered SBP in anesthetized DOCA-salt hypertensive rats (data not shown). Notably, however, SEA0400 did not significantly affect SBP in spontaneously hypertensive rats (SHR) or Wistar Kyoto rats ($P > 0.05$; Fig. 1c). We also examined the antihypertensive effect of SEA0400 in other hypertensive models. SEA0400 significantly decreased SBP in Dahl salt-sensitive rats and SHR when they were chronically loaded with high salt ($P < 0.01$; Fig. 1c). On the other hand, SEA0400 had no effect on SBP in stroke-prone SHR, salt-loaded or salt-unloaded Dahl salt-resistant rats, salt-unloaded Dahl salt-sensitive rats, or two-kidney, one-clip renal hypertensive rats. Thus, SEA0400 selectively suppresses salt-dependent hypertension.

The effect of chronic treatment with SEA0400 was also tested in DOCA-salt hypertensive rats. Administration of SEA0400 (3 or 10 mg/kg) for 3 weeks efficiently overcame the development of hypertension, vascular hypertrophy and renal dysfunction induced by DOCA-salt treatment (**Supplementary Fig. 2** and **Supplementary Tables 1 and 2** online). This suggests that SEA0400 has therapeutic potential as a new antihypertensive drug.

Direct vasodilation by SEA0400

To analyze its antihypertensive mechanism, we infused SEA0400 into the femoral artery of anesthetized DOCA-salt hypertensive rats (Fig. 2a). Intrafemoral infusion of SEA0400 (10 μg/kg/min) markedly increased femoral blood flow (FBF), indicating that SEA0400 caused peripheral vasodilation. A similar infusion did not affect FBF in normotensive sham rats. On the other hand, when the femoral artery of the sham rat (recipient) was crossperfused with aortic blood from the DOCA-salt hypertensive rat (donor), the intrafemoral infusion of SEA0400 significantly increased the FBF ($P < 0.05$; Fig. 2b). SEA0400 had no effect in the crossperfusion between two sham rats. This suggests that humoral vasoconstrictors participate in DOCA-salt hypertension; these vasoconstrictor effects can be antagonized by SEA0400.

Endogenous CTS are thought to contribute to the pathogenesis of salt-sensitive hypertension in patients and experimental animals[7,11–16]. Indeed, chronic administration of ouabain to rats causes hypertension[29,30]. Therefore, we examined the effect of SEA0400 on ouabain-induced hypertension. SEA0400 (1 or 10 mg/kg) suppressed hypertension in a dose-dependent manner in Sprague-Dawley rats on long-term ouabain treatment (Fig. 3a). SEA0400 did not affect the vasopressor responses to intravenous administration of norepinephrine, angiotensin II and endothelin-1 in anesthetized Sprague-Dawley rats (data not shown). Furthermore, to check the antagonistic interaction between ouabain and SEA0400, either ouabain or SEA0400, or both, were infused into the femoral arteries of anesthetized beagles. Intrafemoral infusion of SEA0400 (50 μg/kg/min) alone did not affect FBF. Infusion of either ouabain (0.5 μg/kg/min), however, reduced the FBF by approximately 50%; addition of SEA0400 then restored FBF to the basal level (Fig. 3b).

Effects of SEA0400 on pressurized small arteries

In VSM cells, inhibition of sarcolemmal Na^+/K^+ ATPases by endogenous CTS would be expected to increase $[Na^+]_{cyt}$ and subsequently to raise $[Ca^{2+}]_{cyt}$ through the NCX. To test this hypothesis, we examined the effects of low-dose ouabain and SEA0400 on $[Ca^{2+}]_{cyt}$ (measured as fluo-4 fluorescence) and vasoconstriction in intact, pressurized mouse small mesenteric arteries with myogenic tone. Ouabain (100 nM) increased fluo-4 fluorescence by ~12% and myogenic tone by 20–25% (Fig. 4). The physiological consequences of even small changes are profound because of Poiseuille's law[31]: resistance to blood flow, R, is inversely proportional to the fourth power of the internal radius, r ($R \propto 1/r^4$). Thus, a 5–10% rise in $[Ca^{2+}]_{cyt}$ should augment myogenic tone[32] enough to increase R (and blood pressure)[31] by ~20–50% (Fig. 4).

SEA0400 (300 nM) abolished the effects induced by low-dose ouabain. A video clip of the fluo-4 fluorescence data shown in

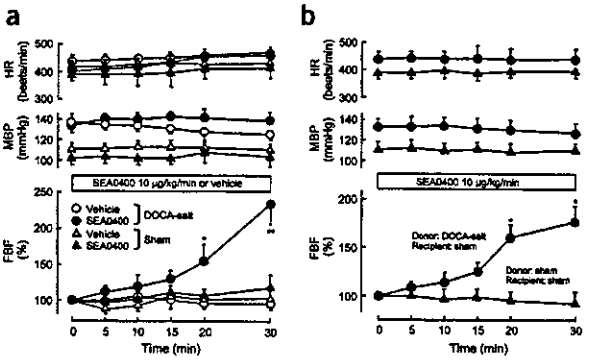

Figure 2 Vascular responses to intrafemoral infusion of SEA0400 in anesthetized DOCA-salt hypertensive or uninephrectomized sham rats. (a) SEA0400 or vehicle was infused at a rate of 20 μl/min into the femoral artery while monitoring the heart rate (HR), mean blood pressure (MBP), and femoral blood flow (FBF). (b) SEA0400 was infused into the femoral artery of the recipient (sham rat) crossperfused with the blood from the donor (DOCA-salt hypertensive rat or sham rat). Bars represent means ± s.e.m. ($n = 4$). $^*P < 0.05$; $^{**}P < 0.01$ compared with pretreatment values.

Figure 4b is available online as **Supplementary Movie 1**. In control arteries, SEA0400 also lowered $[Ca^{2+}]_{cyt}$ slightly (data not shown) and reduced normal myogenic tone by about 10% (Fig. 4c). SEA0400 had no effect on 75 mM K^+-induced vasoconstriction (data not shown), consistent with previous reports on SEA0400 selectivity[27,33]. These results suggest that the increased myogenic tone induced by low-dose ouabain, and even a part of the normal resting tone, may depend upon Ca^{2+} entry mediated by NCX.

Prevention of DOCA-salt hypertension in NCX1 heterozygous mice

To study the functional significance of NCX1 in salt-sensitive hypertension, the hypertensive responsiveness to DOCA-salt treatment was examined in heterozygous NCX1-deficient (*Slc8a1*$^{+/-}$) mice. The NCX1 protein level in the aorta, as well as in other organs[34], of *Slc8a1*$^{+/-}$ mice was about 50% of that seen in wild-type mice (Fig. 5). On the other hand, there were no differences in expression levels of Na^+/K^+-ATPase (α_2 and α_3), L-type Ca^{2+} channel (α_{1C}) and sarcolemmal Ca^{2+}-ATPase in aortas from *Slc8a1*$^{+/-}$ mice (data not shown). Basal SBP of *Slc8a1*$^{+/-}$ mice was no different from that of wild-type mice. DOCA-salt treatment produced a progressive elevation in SBP in wild-type mice ($P < 0.01$), whereas the same treatment did not significantly alter the SBP of *Slc8a1*$^{+/-}$ mice ($P > 0.05$; Fig. 5a). When the sodium level in drinking water for DOCA-salt treatment was increased from 1% to 2%, *Slc8a1*$^{+/-}$ mice responded with a mild increase in SBP (108 ± 3 mmHg ($n = 5$) at 3 weeks, $P < 0.05$), though wild-type mice experienced severe hypertension (128 ± 5 mmHg ($n = 5$), $P < 0.01$). In contrast, hypertensive responses to chronic angiotensin II infusion were similar in *Slc8a1*$^{+/-}$ and wild-type mice (Fig. 5b).

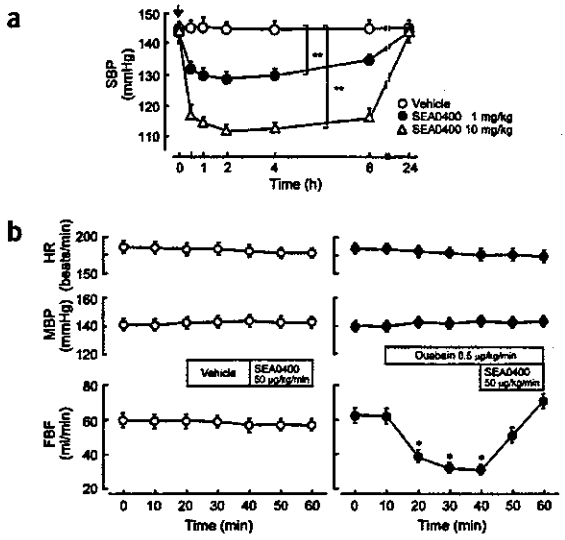

Salt hypersensitivity in VSM-specific NCX1.3 transgenic mice

To test further whether vascular NCX1 has a critical role in salt-sensitive hypertension, we created transgenic mice (*N1.3*$^{Tg/Tg}$) expressing canine *Ncx1.3* driven by the smooth muscle α-actin promoter (Fig. 6a). Southern blotting indicated that four founders had 2–4 copies of the transgene (data not shown). From among them, two independent transgenic lines were selected for detailed study. Western blot analysis showed that NCX1.3 protein was overexpressed in the aortas, but not in the hearts, of these transgenic mice at 6- to 8-fold the level of endogenous NCX1 (Supplementary Fig. 3 online). Immunohistochemical staining indicated dense localization of NCX1.3 in the medial layer of aortas from *N1.3*$^{Tg/Tg}$ mice (Fig. 6b). On the other hand, no difference was observed in protein levels of Na^+/K^+-ATPase (α_2 and α_3), L-type Ca^{2+} channel (α_{1C}) and sarcolemmal Ca^{2+} ATPase in aortas from *N1.3*$^{Tg/Tg}$ mice by western blotting (data not shown). Functional augmentation was correlated with increased NCX1 protein levels in aortas from *N1.3*$^{Tg/Tg}$ mice, as shown by measuring the rate and degree of contraction evoked by Na^+ removal in aortic rings pretreated with ouabain (Supplementary Fig. 3 online). Furthermore, the 10 μM ouabain-induced $[Ca^{2+}]_{cyt}$ rise in mesenteric arteries from *N1.3*$^{Tg/Tg}$ mice was notably greater than in those from wild-type mice (Fig. 6c,d).

Notably, the basal SBP of *N1.3*$^{Tg/Tg}$ mice (103 ± 1.4 mmHg, $n = 6$) was slightly, but significantly ($P < 0.05$), higher than that of wild-type mice (92 ± 1.1 mmHg, $n = 5$). When these mice were fed an 8% NaCl diet with 1% NaCl drinking water, SBP in *N1.3*$^{Tg/Tg}$ mice, but not in wild-type mice, progressively rose to 124 ± 3.5 mmHg ($n = 6$) at 4 weeks after the start of salt loading (Fig. 6e). Oral administration of SEA0400 (10 mg/kg) markedly lowered the SBP of salt-loaded *N1.3*$^{Tg/Tg}$ mice, but not of salt-loaded wild-type mice (Fig. 6f). Intravenous administration of SEA0400 (0.3 mg/kg) also lowered SBP in anesthetized *N1.3*$^{Tg/Tg}$ mice by about 20 mmHg (data not shown). In addition, oral administration of SEA0400 suppressed basal SBP (mild hypertension) of *N1.3*$^{Tg/Tg}$ mice, but not of wild-type mice, and abolished the difference between the two groups (Supplementary Fig. 3 online).

Figure 3 Effects of SEA0400 on ouabain-induced hypertension and vasoconstriction. (a) Recordings over 24 h of SBP after oral administration of SEA0400 in hypertensive rats infused subcutaneously with ouabain (30 μg/kg/d for 5 weeks). $^{**}P < 0.01$ compared with the vehicle group ($n = 5$). (b) Femoral blood flow (FBF) response to intrafemoral infusion of SEA0400 or vehicle at a rate of 0.2 ml/kg/min in the presence (right) or absence (left) of ouabain in anesthetized beagles. MBP and HR were monitored during the experimental periods. $^*P < 0.05$ compared with pretreatment values ($n = 4$).

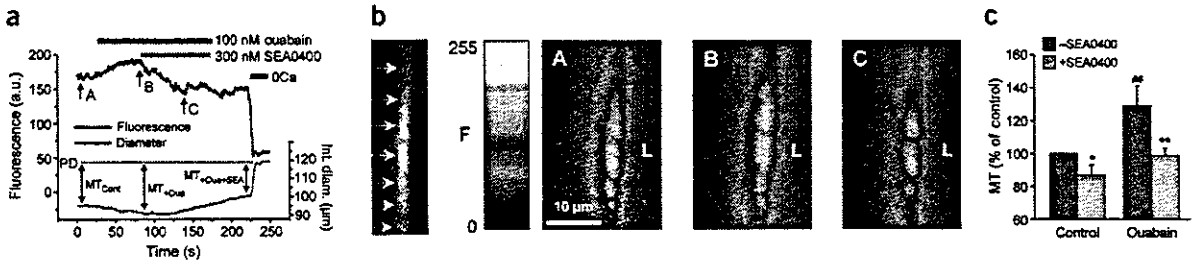

Figure 4 Effects of low-dose ouabain and SEA0400 on cytosolic Ca^{2+} level and myogenic tone (MT) in pressurized mouse small mesenteric arteries. (**a**) Simultaneous recording of fluorescence and internal diameter (Int. diam.) changes in a fluo-4 loaded artery (pressurized to 70 mmHg) by laser confocal microscopy. The fluo-4 fluorescence, indicated in arbitrary units (a.u.), reflects $[Ca^{2+}]_{cyt}$. Periods of exposure to ouabain, SEA0400 and Ca^{2+}-free medium (0Ca) are indicated by colored bars. The dotted line shows the passive internal diameter (PD) in 0Ca. (**b**) Fluorescent image on the left shows individual myocytes loaded with fluo-4 (arrows); the artery has only a single layer of myocytes. Pseudocolor images (**A–C**) indicate the relative $[Ca^{2+}]_{cyt}$ at the times shown in **a**. L, artery lumen. A video clip of the original data from this experiment is available at **Supplementary Movie 1** online. (**c**) Summary of the effects of ouabain and SEA0400 on MT, normalized to MT under control conditions. Mean PD was 107 ± 4 μm. At 70 mmHg, arteries constricted to 77 ± 4 μm internal diameter (= control MT). Ouabain caused a further constriction to 70 ± 4 μm; based on Poiseuille's law[31], this should increase resistance to blood flow (and blood pressure) by ~46%. $^{*}P < 0.05$; $^{**}P < 0.01$ versus pretreatment values ('–SEA0400'). $^{\#\#}P < 0.01$ versus control values ($n = 6$).

To verify that the antihypertensive effect of SEA0400 results from the inhibition of genetically overexpressed NCX1.3, we generated transgenic mice (*mN1.3*$^{Tg/Tg}$) expressing an SEA0400-insensitive G833C mutant[28] (Fig. 6a). Three independent lines of *mN1.3*$^{Tg/Tg}$ mice were selected for detailed analysis. The phenotypes of *mN1.3*$^{Tg/Tg}$ mice were very similar to those of *N1.3*$^{Tg/Tg}$ mice, except for their vascular response to SEA0400 (Fig. 6b–e and Supplementary Fig. 3 online); this drug blocked the contraction evoked by Na^+ removal in ouabain-pretreated aortic rings and the ouabain-induced $[Ca^{2+}]_{cyt}$ rise in arterial strips from *N1.3*$^{Tg/Tg}$ mice, but not from *mN1.3*$^{Tg/Tg}$ mice. In *mN1.3*$^{Tg/Tg}$ mice, SEA0400 (10 mg/kg) did not show a reduction in high salt–induced hypertension (Fig. 6f) and basal SBP (Supplementary Fig. 3 online). This shows that SEA0400 acts on the overexpressed NCX1.3 in VSM cells.

Given the possibility of nonspecific effects associated with NCX1 overexpression, as a further control we generated transgenic mice (*N1.1*$^{Tg/Tg}$) expressing canine *Ncx1.1* driven by the α-myosin heavy-chain promoter. In established *N1.1*$^{Tg/Tg}$ lines, hearts, but not aortas, showed a 2- to 3-fold increase in the level of NCX1 protein. Basal SBP of *N1.1*$^{Tg/Tg}$ mice was normal, and was similar to that of wild-type mice. Furthermore, the blood pressure of *N1.1*$^{Tg/Tg}$ mice, like that of wild-type mice, was resistant to long-term salt-loading and insensitive to the effect of SEA0400 (Supplementary Fig. 4 online).

DISCUSSION

The critical importance of sodium retention, resulting from excess salt intake or reduced renal salt excretion, in the pathogenesis of hypertension is widely recognized[3–6]. But the molecular mechanisms underlying salt-sensitive hypertension remain obscure. Here we show that SEA0400 lowers arterial blood pressure in various models of salt-dependent hypertension. SEA0400 does not, however, affect arterial blood pressure in normotensive rats or in other types of hypertensive rats. Furthermore, NCX1 heterozygous mice are resistant to DOCA-salt hypertension, but not to angiotensin II–induced hypertension. These findings suggest that vascular NCX1 is critical in the development of salt-sensitive hypertension.

The contraction of VSM cells is initiated by a rise in $[Ca^{2+}]_{cyt}$ through voltage-gated or receptor-operated Ca^{2+} channels in the sarcolemma, or both, or through Ca^{2+}-release channels in the sarcoplasmic reticulum membrane[35,36]. In general, sarcolemmal NCX, like the sarcolemmal or sarcoplasmic reticulum Ca^{2+}ATPases, is thought to contribute to Ca^{2+} extrusion from the cytosol in the relaxation process. Data obtained using antisense oligonucleotides indicate that NCX1 knockdown prolongs agonist responses by delaying the return of $[Ca^{2+}]_{cyt}$ to the resting level in cultured VSM cells[37,38].

To confirm the *in vivo* function of vascular NCX1 in mice, we generated VSM-specific transgenic mice expressing either wild-type NCX1.3 (*N1.3*$^{Tg/Tg}$) or the SEA0400-insensitive G833C mutant (*mN1.3*$^{Tg/Tg}$). Comparative experiments using these mutants and SEA0400 are useful for assessing the pharmacological significance of NCX inhibition[28]. Interestingly, both kinds of transgenic mice were mildly hypertensive (by about 10 mmHg) compared with wild-type mice. They also exhibited high salt–induced hypertension as a result of increased salt sensitivity. Administration of SEA0400 normalized

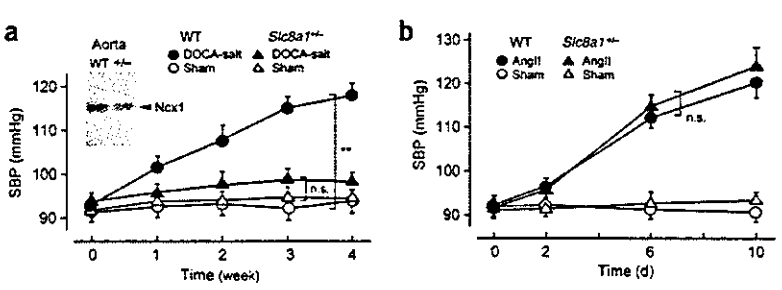

Figure 5 Prevention of DOCA-salt hypertension in *Slc8a1*$^{+/-}$ mice. (**a**) Uninephrectomized *Slc8a1*$^{+/-}$ and wild-type (WT) mice received DOCA (75 mg/kg) subcutaneously twice a week, and were given tap water containing 1% NaCl for 4 weeks. Sham mice were uninephrectomized but not given DOCA and salt. (**b**) Miniosmotic pumps containing angiotensin II (AngII) or vehicle (sham) were subcutaneously implanted in *Slc8a1*$^{+/-}$ and WT mice on day 0. Systolic blood pressure (SBP) was monitored by tail cuff. $^{**}P < 0.01$ versus control groups ($n = 5$ or 6).

blood pressure and suppressed salt-dependent hypertension in $N1.3^{Tg/Tg}$ mice, but not in $mN1.3^{Tg/Tg}$ mice. The latter mutation interferes with SEA0400 binding but does not affect Na^+/Ca^{2+} exchange[28]. In contrast, heart-specific transgenic mice expressing NCX1.1 were salt-insensitive, and their blood pressure did not respond to SEA0400. These results indicate that vascular NCX1 acts primarily as a Ca^{2+} entry pathway for regulating arterial tone, especially under sodium-retaining conditions. SEA0400 exerts its antihypertensive effect by blocking this Ca^{2+} entry in arterial myocytes.

Indeed, SEA0400 reverses the vasoconstriction and hypertension induced by exogenous ouabain, which may facilitate Ca^{2+} entry through NCX due to elevated $[Na^+]_{cyt}$, although SEA0400 does not directly affect the activity of Na^+/K^+-ATPases[27]. Notably, in VSM cells the NCX1 is colocalized with Na^+/K^+-ATPase α_2 and α_3 isoforms, which have high affinity for ouabain[39], in plasma membrane microdomains adjacent to the sarcoplasmic reticulum[40,41]. Functional coupling between NCX and Na^+/K^+-ATPase has been reported in vascular and cardiac myocytes[37,42–44]. As described above, endogenous plasma CTS are increased under pathological conditions such as salt-sensitive hypertension[7,11–16]. When CTS inhibit Na^+/K^+-ATPases (α_2 and α_3) in VSM cells, the elevation of local Na^+ in the submembrane area is expected to facilitate Ca^{2+} entry through NCX1, resulting in vasoconstriction. Our data indicate that blood from DOCA-salt hypertensive rats contains humoral vasoconstrictors whose action is counteracted by SEA0400. Also, using isolated, pressurized mouse small mesenteric arteries, we confirmed that 100 nM ouabain increases both $[Ca^{2+}]_{cyt}$ and myogenic tone by about 20–25% and that SEA0400 completely abolishes these effects. In addition, the 10 μM ouabain–induced $[Ca^{2+}]_{cyt}$ rise in arterial strips from transgenic mice was greater than in those from wild-type mice. SEA0400 blocked these $[Ca^{2+}]_{cyt}$ rises in $N1.3^{Tg/Tg}$ and wild-type mice, but not in $mN1.3^{Tg/Tg}$ mice. These data provide evidence that ouabain triggers Ca^{2+} entry through NCX1 in VSM cells by inhibiting high ouabain–affinity Na^+ pumps (α_2 or α_3) and elevating submembrane Na^+. Although ouabain has also been reported to mediate other signaling pathways[45], they apparently are not involved in the VSM mechanism described here.

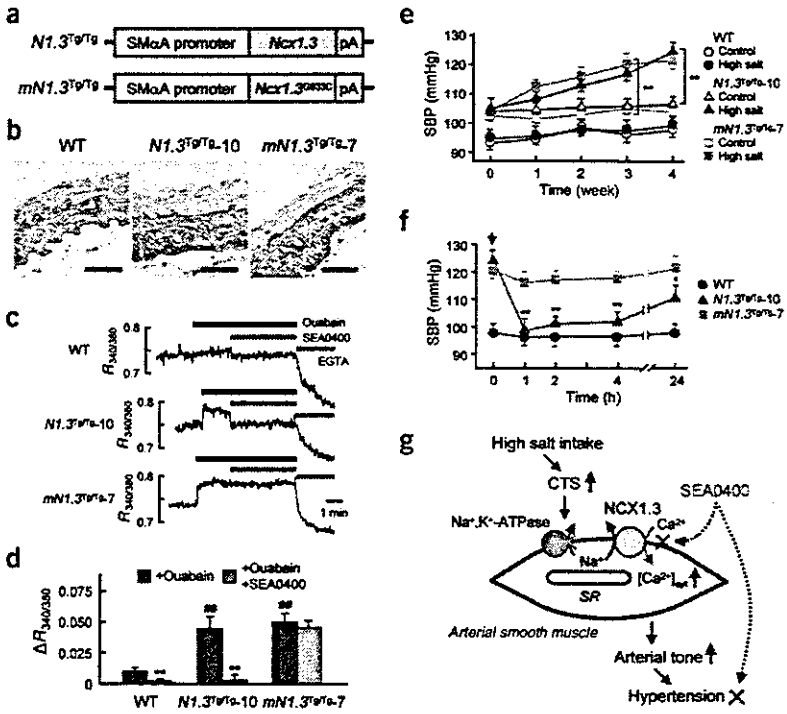

Figure 6 Enhanced salt-sensitivity in $N1.3^{Tg/Tg}$ or $mN1.3^{Tg/Tg}$ mice. (a) Schematic representation of the transgene used to generate VSM-specific transgenic mice. The *Ncx1.3* or its G833C mutant (*Ncx1.3*^{G833C}) was brought under the control of human smooth muscle α-actin (SMαA) promoter. (b) Immunohistochemical localization of NCX1 proteins in the medial layer of thoracic aortas from wild-type (WT) mice and two representative transgenic lines ($N1.3^{Tg/Tg}$-10 and $mN1.3^{Tg/Tg}$-7). Scale bars, 50 μm. (c) Effects of ouabain and SEA0400 on $[Ca^{2+}]_{cyt}$ (fura-PE3 fluorescence ratio ($R_{340/380}$)) in isolated mesenteric arteries from transgenic and WT mice. Periods of exposure to 10 μM ouabain, 1 μM SEA0400 and 4 mM EGTA are indicated by bars. All experiments were performed in the presence of 10 μM nicardipine to suppress L-type Ca^{2+} channels. (d) Summary of the experiments shown in (c). $^{**}P < 0.01$ versus pretreatment values ('+Ouabain'). $^{\#\#}P < 0.01$ versus WT groups ($n = 5$). (e,f) Salt-induced hypertension and antihypertensive effects of SEA0400 (10 mg/kg) in transgenic and WT mice treated with a high-salt diet (8% NaCl) and tap water containing 1% NaCl for 4 weeks. $^{*}P < 0.05$; $^{**}P < 0.01$ ($n = 5$ or 6). (g) Proposed pathway responsible for salt-sensitive hypertension. High salt intake causes the levels of endogenous CTS to rise in the plasma. This results in the increase in subplasma membrane $[Na^+]$ of arterial smooth muscle. The restricted $[Na^+]$ accumulation elevates $[Ca^{2+}]_{cyt}$ by vascular NCX1 isoform–mediated Ca^{2+} entry. This enhances arterial tone and causes hypertension. SEA0400 blocks this Ca^{2+} entry and exerts an antihypertensive effect in salt-sensitive hypertension.

SEA0400 does not affect arterial blood pressure in normotensive or salt-independent hypertensive animals. Intrafemoral infusion of SEA0400 in normal rats and beagles does not change arterial blood flow unless the arteries are perfused with exogenous ouabain or aortic blood from salt-dependent hypertensive animals. In addition, NCX1 heterozygous mice maintain normal blood pressure. Thus, the Ca^{2+} entry mode of NCX1 in VSM cells apparently has little role in blood pressure control in normotensive or in salt-insensitive hypertensive animals, probably owing to low plasma levels of CTS and to the overriding effects of reflex regulatory mechanisms. Nevertheless, the Ca^{2+} entry mode of NCX1 could have a role in regional blood flow even in normotensive and salt-insensitive animals, because SEA0400 slightly suppresses basal myogenic tone with a small reduction of $[Ca^{2+}]_{cyt}$ in pressurized mouse small mesenteric arteries.

In conclusion, our results show that the Ca^{2+} entry mode of vascular NCX1 is involved in the contractile regulation of small arteries and in the development of salt-dependent hypertension. Notably, recent human genome-wide linkage analysis of genes that affect blood pressure identified four regions, one of which includes *SLC8A1*, as loci containing candidate genes that influence blood pressure[46]. In humans and animals, endogenous CTS levels increase in plasma during salt retention[7,11–16]. Inhibition of Na^+ pumps by CTS should elevate local Na^+ and, through NCX1, $[Ca^{2+}]_{cyt}$ in VSM cells, thereby

promoting vasoconstriction (Fig. 6g). In this pathway, vascular NCX1 is a key mediator. SEA0400 selectively blocks NCX1.3, the vascular isoform of NCX1, and suppresses salt-dependent hypertension and associated secondary organ damage. Thus, the Ca^{2+} entry mode of vascular NCX1 may be a useful target for the development of therapies for salt-sensitive hypertension. Indeed, response to inhibitors of NCX1 may be diagnostic for salt-sensitive hypertension and involvement of the pathway illustrated in Figure 6g.

METHODS

$^{45}Ca^{2+}$ uptake. To examine the splice isoform selectivity of SEA0400, we cloned *NCX1.1, NCX1.3, NCX1.4, NCX1.6* and *NCX1.7* into pcDNA3.1 (Invitrogen) by PCR using human aortic cDNAs (Clontech). We transfected these plasmids with Lipofectin (Invitrogen) into CCL39 fibroblasts and we selected cells stably expressing NCX1 using a Ca^{2+}-killing procedure[47]. Intracellular Na^+-dependent $^{45}Ca^{2+}$ uptake into cells was assayed as described[47] (see Supplementary Methods online).

Experimental hypertensive models. To produce DOCA-salt hypertensive animals, 5-week-old male Sprague-Dawley rats or 12-week-old male mice were unilaterally nephrectomized under anesthesia with sodium pentobarbital. After allowing the animals a 1-week recovery, we administered DOCA (15 mg/kg for rats or 75 mg/kg for mice) with corn oil subcutaneously twice a week for 4 weeks. These animals then drank tap water containing 1% NaCl. Control animals (sham) were uninephrectomized but not given DOCA and salt. In the preparation of two-kidney, one-clip renal hypertensive rats, we anesthetized male Sprague-Dawley rats with sodium pentobarbital, and partially occluded the left renal artery by a silver clip (0.2 mm in diameter) for 4 weeks. To produce ouabain-induced hypertension, we infused ouabain subcutaneously at a rate of 30 μg/kg/day into male Sprague-Dawley rats by miniosmotic pumps (ALZET 2002) for 5 weeks. Ouabain was dissolved in sterile phosphate-buffered saline. To produce angiotensin II–induced hypertension, we subcutaneously implanted miniosmotic pumps containing either vehicle (0.01 N acetic acid in saline solution) or angiotensin II (750 μg/kg/d for 10 d) in male mice. We measured SBP at room temperature by a tail cuff method using an MK2000 blood pressure monitor (Muromachi Kikai). Rats or mice were acclimated to the procedures of blood pressure measurement for a week preceding actual data collection. We administered SEA0400 orally or intravenously with 5% gum arabic or a lipid emulsion containing 20% soybean oil (vehicle), respectively.

Intrafemoral infusion. To determine the peripheral vasodilation, we infused SEA0400 (10 μg/kg/min) or vehicle at a rate of 20 μl/min through a polyethylene tube in the right femoral artery of DOCA-salt hypertensive rats or uninephrectomized sham rats, anesthetized with sodium pentobarbital. In other experiments, we infused SEA0400 into the right femoral artery of the sham rat (recipient), which was crossperfused with vena caval and aortic blood of the donor rat and stabilized for 30 min. In yet other experiments, we infused SEA0400 (50 μg/kg/min) alone or in combination with ouabain (0.5 μg/kg/min) at a rate of 0.2 ml/min into the left femoral artery of anesthetized male beagles (9–10 kg). In all these experiments, FBF, systemic blood pressure and heart rate were monitored directly with a square-wave flowmeter and a pressure transducer (Nihon Koden), respectively.

Transgenic mice. We constructed the transgene by inserting canine *Ncx1.3* or its G833C mutant[28] between the human smooth muscle α-actin promoter and the SV40 polyadenylation sequence of the plasmid (T. Miwa). We also prepared an additional transgene by inserting canine *Ncx1.1* between the mouse α-myosin heavy chain promoter and the SV40 polyadenylation sequence of the plasmid (J. Robbins). Each transgene was microinjected into the pronuclei of fertilized C57BL/6J mouse embryos at the single-cell stage. We implanted the embryos into pseudopregnant foster mothers. Positive transgenic mice were identified as described[34]; mice were bred to homozygosity.

Imaging of small mesenteric arteries. Diameter measurement and Ca^{2+} imaging of mouse mesenteric artery were performed as described[48]. Distal mesenteric arteries (2–3 mm length, 120–150 μm passive external diameter) from male C57BL/6J mice were cannulated at both ends and continuously superfused with gassed Krebs solution (37 °C, 70 mmHg) to induce myogenic tone. For measurement of diameter only, the artery outer diameter was continuously monitored by a real-time edge-detection system (National Instruments). For Ca^{2+} imaging, arterial segments were loaded with 15 μM fluo-4-AM for ~3 h. We imaged dye-loaded arteries with a confocal imaging system (Nipkow-Yokogawa dual spinning disk, Solamere Technology) connected to a Nikon Eclipse 2000 microscope equipped with a water immersion objective (×60). Images were captured at the rate of 2–4 frames/s.

Other procedures and materials. Immunoblotting for membrane proteins and immunohistochemistry of frozen sections were performed as described[47,49], with some modifications. We performed analyses of aortic morphology and renal function as described[50]. We also performed measurements of contraction in aortic rings and $[Ca^{2+}]_{cyt}$ (fura-PE3 fluorescence ratio; $R_{340/380}$) in arterial strips as described[34,38], with some modifications (see Supplementary Methods online). We used an unpaired *t*-test, one-way ANOVA followed by Dunnett's test or two-way ANOVA for statistical analyses. Values of $P < 0.05$ were considered statistically significant. SEA0400 (2-[4-[(2,5-difluorophenyl)methoxy]phenoxy]-5-ethoxyaniline) was synthesized by Taisho Pharmaceutical Co. Ltd.

Animal regulations. We used all animals in accordance with the Guidelines for Animal Experiments in Fukuoka University and the US National Institutes of Health Guide for the Care and Use of Laboratory Animals.

Note: Supplementary information is available on the Nature Medicine website.

ACKNOWLEDGMENTS

We thank K. Takahashi and S. Okuyama (Taisho Pharmaceutical Co. Ltd.), K. Saku and H. Urata (Fukuoka University), J. Kimura (Fukushima Medical University) and Y. Matsumura (Osaka University of Pharmaceutical Sciences) for discussions, and W.G. Wier and R. Saunders (University of Maryland) for help in making the video clip. This work was supported by Grants-in-Aid for scientific research (14570097, 16590213) from the Ministry of Education, Science and Culture of Japan, a grant from the Salt Science Research Foundation (No.02), US National Institutes of Health grant HL-45215, and an American Heart Association Mid-Atlantic Affiliate Postdoctoral Fellowship.

COMPETING INTERESTS STATEMENT

The authors declare that they have no competing financial interests.

Received 20 May; accepted 8 September 2004
Published online at http://www.nature.com/naturemedicine/

1. Mosterd, A. *et al.* Trends in the prevalence of hypertension, antihypertensive therapy, and left ventricular hypertrophy from 1950 to 1989. *N. Engl. J. Med.* **340**, 1221–1227 (1999).
2. Kannel, W.B. Elevated systolic blood pressure as a cardiovascular risk factor. *Am. J. Cardiol.* **85**, 251–255 (2000).
3. Cowley, A.W. Long-term control of arterial blood pressure. *Physiol. Rev.* **72**, 231–300 (1992).
4. Blaustein, M.P. Physiological effects of endogenous ouabain: control of intracellular calcium stores and cell responsiveness. *Am. J. Physiol.* **264**, C1367–C1387 (1993).
5. Haddy, F.J. & Pamnani, M.B. Role of dietary salt in hypertension. *J. Am. Coll. Nutr.* **14**, 428–438 (1995).
6. Lifton, R.P., Gharavi, A.G. & Geller, D.S. Molecular mechanisms of human hypertension. *Cell* **104**, 545–556 (2001).
7. Hamlyn, J.M. *et al.* Identification and characterization of a ouabain-like compound from human plasma. *Proc. Natl. Acad. Sci. USA* **88**, 6259–6263 (1991).
8. Schneider, R. *et al.* Bovine adrenals contain, in addition to ouabain, a second inhibitor of the sodium pump. *J. Biol. Chem.* **273**, 784–792 (1998).
9. Bagrov, A.Y. *et al.* Characterization of a urinary bufodienolide Na^+,K^+-ATPase inhibitor in patients after acute myocardial infarction. *Hypertension* **31**, 1097–1103 (1998).
10. Schoner, W. Endogenous cardiac glycosides, a new class of steroid hormones. *Eur. J. Biochem.* **269**, 2440–2448 (2002).
11. Hamlyn, J.M. *et al.* A circulating inhibitor of $(Na^+ + K^+)$-ATPase associated with essential hypertension. *Nature* **300**, 650–652 (1982).
12. Hasegawa, T., Masugi, F., Ogihara, T. & Kumahara, Y. Increase in plasma ouabain-like inhibitor of Na^+,K^+-ATPase with high sodium intake in patients with essential hypertension. *J. Clin. Hypertens.* **3**, 419–429 (1987).
13. Hamlyn, J.M., Hamilton, B.P. & Manunta, P. Endogenous ouabain, sodium balance and blood pressure: a review and a hypothesis. *J. Hypertens.* **14**, 151–167 (1996).

14. Manunta, P. *et al.* Left ventricular mass, stroke volume, and ouabain-like factor in essential hypertension. *Hypertension* **34**, 450–456 (1999).
15. Goto, A. & Yamada, K. Putative roles of ouabainlike compound in hypertension: revisited. *Hypertens. Res.* **23**, S7–S13. (2000).
16. Fedorova, O.V., Lakatta, E.G. & Bagrov, A.Y. Endogenous Na,K pump ligands are differentially regulated during acute NaCl loading of Dahl rats. *Circulation* **102**, 3009–3014 (2000).
17. Ferrari, P. *et al.* PST2238: a new antihypertensive compound that antagonizes the long-term pressor effect of ouabain. *J. Pharmacol. Exp. Ther.* **285**, 83–94 (1998).
18. Takahashi, H. Endogenous digitalislike factor: an update. *Hypertens. Res.* **23**, S1–S5 (2000).
19. Blaustein, M.P. Sodium ions, calcium ions, blood pressure regulation, and hypertension: a reassessment and a hypothesis. *Am. J. Physiol.* **232**, C165–C173 (1977).
20. Philipson, K.D. & Nicoll, D.A. Sodium-calcium exchange: a molecular perspective. *Annu. Rev. Physiol.* **62**, 111–133. (2000).
21. Nakasaki, Y., Iwamoto, T., Hanada, H., Imagawa, T. & Shigekawa, M. Cloning of the rat aortic smooth muscle Na^+/Ca^{2+} exchanger and tissue-specific expression of isoforms. *J. Biochem.* **114**, 528–534 (1993).
22. Lee, S.L., Yu, A.S. & Lytton, J. Tissue-specific expression of Na^+-Ca^{2+} exchanger isoforms. *J. Biol. Chem.* **269**, 14849–14852 (1994).
23. Quednau, B.D., Nicoll, D.A. & Philipson, K.D. Tissue specificity and alternative splicing of the Na^+/Ca^{2+} exchanger isoforms NCX1, NCX2, and NCX3 in rat. *Am. J. Physiol.* **272**, C1250–C1261 (1997).
24. Bers, D.M. Cardiac excitation-contraction coupling. *Nature* **415**, 198–205 (2002).
25. Blaustein, M.P. & Lederer, W.J. Sodium/calcium exchange: its physiological implications. *Physiol. Rev.* **79**, 763–854 (1999).
26. Shigekawa, M. & Iwamoto, T. Cardiac Na^+-Ca^{2+} exchange: molecular and pharmacological aspects. *Circ. Res.* **88**, 864–876 (2001).
27. Matsuda, T. *et al.* SEA0400, a novel and selective inhibitor of the Na^+-Ca^{2+} exchanger, attenuates reperfusion injury in the in vitro and in vivo cerebral ischemic models. *J. Pharmacol. Exp. Ther.* **298**, 249–256 (2001).
28. Iwamoto, T. *et al.* Molecular determinants of Na^+/Ca^{2+} exchange (NCX1) inhibition by SEA0400. *J. Biol. Chem.* **279**, 7544–7553 (2004).
29. Yuan, C.M. *et al.* Long-term ouabain administration produces hypertension in rats. *Hypertension* **22**, 178–187 (1993).
30. Manunta, P., Rogowski, A.C., Hamilton, B.P. & Hamlyn, J.M. Ouabain-induced hypertension in the rat: relationships among plasma and tissue ouabain and blood pressure. *J. Hypertens.* **12**, 549–560 (1994).
31. Berne, R.M. & Levy, M.N. Chapter V. Hemodynamics. in *Cardiovascular Physiology* edn. 8 (eds. Berne, R.M. & Levy, M.N.) 115–134 (Mosby, St. Louis, 2001).
32. Knot, H.J. & Nelson, M.T. Regulation of arterial diameter and wall $[Ca^{2+}]$ in cerebral arteries of rat by membrane potential and intravascular pressure. *J. Physiol.* **508**, 199–209 (1998).
33. Tanaka, H. *et al.* Effect of SEA0400, a novel inhibitor of sodium-calcium exchanger, on myocardial ionic currents. *Br. J. Pharmacol.* **135**, 1096–1100 (2002).
34. Wakimoto, K. *et al.* Targeted disruption of Na^+/Ca^{2+} exchanger gene leads to cardiomyocyte apoptosis and defects in heartbeat. *J. Biol. Chem.* **275**, 36991–36998 (2000).
35. Berridge, M.J., Bootman, M.D. & Roderick, H.L. Calcium signalling: dynamics, homeostasis and remodelling. *Nat. Rev. Mol. Cell Biol.* **4**, 517–529 (2003).
36. Poburko, D., Kuo, K.H., Dai, J., Lee, C.H. & van Breemen, C. Organellar junctions promote targeted Ca^{2+} signaling in smooth muscle: why two membranes are better than one. *Trends Pharmacol. Sci.* **25**, 8–15 (2004).
37. Slodzinski, M.K., Juhaszova, M. & Blaustein, M.P. Antisense inhibition of Na^+/Ca^{2+} exchange in primary cultured arterial myocytes. *Am. J. Physiol.* **269**, C1340–C1345 (1995).
38. Slodzinski, M.K. & Blaustein, M.P. Physiological effects of Na^+/Ca^{2+} exchanger knockdown by antisense oligodeoxynucleotides in arterial myocytes. *Am. J. Physiol.* **275**, C251–C259 (1998).
39. Sweadner, K.J. Isozymes of the Na^+/K^+-ATPase. *Biochim. Biophys. Acta.* **988**, 185–220 (1989).
40. Moore, E.D. *et al.* Coupling of the Na^+/Ca^{2+} exchanger, Na^+/K^+ pump and sarcoplasmic reticulum in smooth muscle. *Nature* **365**, 657–660 (1993).
41. Juhaszova, M. & Blaustein, M.P. Distinct distribution of different Na^+ pump α subunit isoforms in plasmalemma. Physiological implications. *Ann. N.Y. Acad. Sci.* **834**, 524–536 (1997).
42. Fujioka, Y., Matsuoka, S., Ban, T. & Noma, A. Interaction of the Na^+-K^+ pump and Na^+-Ca^{2+} exchange via $[Na^+]_i$ in a restricted space of guinea-pig ventricular cells. *J. Physiol.* **509**, 457–470 (1998).
43. Arnon, A., Hamlyn, J.M. & Blaustein, M.P. Ouabain augments Ca^{2+} transients in arterial smooth muscle without raising cytosolic Na^+. *Am. J. Physiol.* **279**, H679–H691 (2000).
44. Reuter, H. *et al.* The Na^+-Ca^{2+} exchanger is essential for the action of cardiac glycosides. *Circ. Res.* **90**, 305–308 (2002).
45. Aizman, O., Uhlen, P., Lal, M., Brismar, H. & Aperia, A. Ouabain, a steroid hormone that signals with slow calcium oscillations. *Proc. Natl. Acad. Sci. USA* **98**, 13420–13424 (2001).
46. Krushkal, J. *et al.* Genome-wide linkage analyses of systolic blood pressure using highly discordant siblings. *Circulation* **99**, 1407–1410 (1999).
47. Iwamoto, T., Pan, Y., Nakamura, T.Y., Wakabayashi, S. & Shigekawa, M. Protein kinase C-dependent regulation of Na^+/Ca^{2+} exchanger isoforms NCX1 and NCX3 does not require their direct phosphorylation. *Biochemistry* **37**, 17230–17238 (1998).
48. Zhang, J., Wier, W.G. & Blaustein, M.P. Mg^{2+} blocks myogenic tone but not K^+-induced constriction: role for SOCs in small arteries. *Am. J. Physiol.* **283**, H2692–H2705 (2002).
49. Yamashita, J. *et al.* Attenuation of ischemia/reperfusion-induced renal injury in mice deficient in Na^+/Ca^{2+} exchanger. *J. Pharmacol. Exp. Ther.* **304**, 284–293 (2003).
50. Matsumura, Y. *et al.* Exaggerated vascular and renal pathology in endothelin-B receptor-deficient rats with deoxycorticosterone acetate-salt hypertension. *Circulation* **102**, 2765–2773 (2000).

The Journal of Cell Biology

Article

A novel LIM protein Cal promotes cardiac differentiation by association with CSX/NKX2-5

Hiroshi Akazawa,[1] Sumiyo Kudoh,[2] Naoki Mochizuki,[3] Noboru Takekoshi,[2] Hiroyuki Takano,[1] Toshio Nagai,[1] and Issei Komuro[1]

[1]Department of Cardiovascular Science and Medicine, Chiba University Graduate School of Medicine, Chiba 260-8670, Japan
[2]Department of Cardiology, Kanazawa Medical University, Ishikawa 920-0265, Japan
[3]Department of Structural Analysis, National Cardiovascular Center Research Institute, Osaka 565-8565, Japan

The cardiac homeobox transcription factor CSX/NKX2-5 plays an important role in vertebrate heart development. Using a yeast two-hybrid screening, we identified a novel LIM domain–containing protein, named CSX-associated LIM protein (Cal), that interacts with CSX/NKX2-5. CSX/NKX2-5 and Cal associate with each other both in vivo and in vitro, and the LIM domains of Cal and the homeodomain of CSX/NKX2-5 were necessary for mutual binding. Cal itself possessed the transcription-promoting activity, and cotransfection of Cal enhanced CSX/NKX2-5–induced activation of *atrial natriuretic peptide* gene promoter. Cal contained a functional nuclear export signal and shuttled from the cytoplasm into the nucleus in response to calcium. Accumulation of Cal in the nucleus of P19CL6 cells promoted myocardial cell differentiation accompanied by increased expression levels of the target genes of CSX/NKX2-5. These results suggest that a novel LIM protein Cal induces cardiomyocyte differentiation through its dynamic intracellular shuttling and association with CSX/NKX2-5.

Introduction

CSX/NKX2-5 is a member of NK homeobox gene family that is conserved in evolution and acts as a DNA-binding transcription activator (Komuro and Izumo, 1993; Lints et al., 1993; Akazawa and Komuro, 2003). During embryogenesis, *CSX/NKX2-5* is expressed predominantly in the heart progenitor cells from the very early stage. Targeted disruption of murine *CSX/NKX2-5* resulted in embryonic lethality due to the arrested looping morphogenesis of the heart tube (Lyons et al., 1995). In addition, mutations of *CSX/NKX2-5* cause human hereditary cardiac malformations associated with atrioventricular conduction disturbance (Schott et al., 1998). These results indicate that *CSX/NKX2-5* plays a pivotal role in normal heart development in mammals.

To understand the mechanisms of how *CSX/NKX2-5* controls cardiac development, it is necessary to elucidate the molecular framework of fine-tuned transcriptional regulation of its distinct target genes. Recently, protein–protein interactions have been recognized to be important in many biological processes. Protein complexes consisting of transcription factors and cofactors are responsible for transcriptional regulation, and its composition is thought to be the key determinant of specificity and intensity of the reaction. Transcriptional activity of CSX/NKX2-5 is modulated through physical interaction with other transcription factors such as GATA-4 (Durocher et al., 1997; Lee et al., 1998; Shiojima et al., 1999), SRF (Chen and Schwartz, 1996), and Tbx-5 (Bruneau et al., 2001; Hiroi et al., 2001). Here, we isolated a novel CSX/NKX2-5–associated protein by a yeast two-hybrid screening using *CSX/NKX2-5* as a bait. The protein was a novel LIM domain–containing protein, which we named CSX-associated LIM protein (*Cal*). The LIM domain is a double-zinc finger motif and functions as a module for protein–protein interactions (Dawid et al., 1998; Bach, 2000). Nuclear LIM proteins such as LIM homeodomain proteins and LIM only proteins are directly involved in transcriptional regulation during cell differentiation (Dawid et al., 1998; Bach, 2000). Cytoplasmic LIM proteins are involved in divergent biological processes such as regulation of cytoarchitecture, protein trafficking, and specification of cell polarity (Dawid et al., 1998; Bach,

Address correspondence to Issei Komuro, Dept. of Cardiovascular Science and Medicine, Chiba University Graduate School of Medicine, 1-8-1 Inohana, Chuo-ku, Chiba 260-8670, Japan. Tel.: 81-43-226-2097. Fax: 81-43-226-2557. email: komuro-tky@umin.ac.jp

Key words: cardiogenesis; homeobox transcription factor; LIM domain; nucleocytoplasmic transport; transcriptional regulation

Abbreviations used in this paper: ANP, atrial natriuretic peptide; Ca^{2+}, calcium; Cal, CSX-associated LIM protein; CRP, cysteine-rich protein; LMB, leptomycin B; LPP, lipoma preferred partner; NES, nuclear export signal; SERCA2, sarcoplasmic reticulum Ca^{2+}-ATPase 2; trip6, thyroid receptor interacting protein 6.

The Journal of Cell Biology, Volume 164, Number 3, February 2, 2004 395–405
http://www.jcb.org/cgi/doi/10.1083/jcb.200309159

2000). In regard to muscle development, the roles of cysteine-rich protein (CRP) 3/MLP, which is primarily cytoplasmic, have attracted much attention (Arber et al., 1994). Overexpression of CRP3/MLP in C2C12 myoblasts promoted skeletal myogenesis, whereas inhibition of CRP3/MLP activity by antisense oligonucleotide interrupted terminal differentiation of these cells. Mice homozygous for CRP3/MLP mutation exhibited dilated cardiomyopathy resulted from disrupted cytoarchitecture in cardiomyocytes (Arber et al., 1997). These results indicate the possibility that cytoplasmic LIM proteins regulate cell differentiation as well. Recently, some cytoplasmic LIM proteins have been reported to show nuclear localization. For example, CRP3/MLP associates with nuclear LIM proteins Lmo1 and Apterous (Arber and Caroni, 1996) and basic helix-loop-helix transcription factor MyoD (Kong et al., 1997) as well as cytoskeletal proteins, Zyxin, and α actinin (Louis et al., 1997). However, the molecular mechanism by which the cytoplasmic LIM proteins are involved in nuclear events remains largely unknown.

Here, we show that Cal functions as a coactivator for CSX/NKX2-5 and fulfills its cooperative function based on its dynamic intracellular shuttling mechanisms. Consistent with the notion that the LIM domains function as an interface of protein–protein interactions, the LIM domains of Cal are required for binding to the homeodomain of CSX/NKX2-5. Cal itself has the transcription-promoting activity and activates the *atrial natriuretic peptide* (*ANP*) promoter by forming complex with CSX/NKX2-5. Cal traffics out of the nucleus by nuclear export signal (NES)–dependent mechanisms and traffics into the nucleus in response to an increase of intracellular calcium (Ca^{2+}) concentration. Nuclear expression of Cal promotes cardiac differentiation of P19CL6 cells in vitro. Characterization of complex formation between CSX/NKX2-5 and Cal will provide a unique framework whereby gene expression during cardiogenesis is fine-tuned by the primarily cytoplasmic LIM proteins that were supposed to be involved in cytoskeletal organization.

Results

Molecular cloning and characterization of Cal

To identify proteins that interact with CSX/NKX2-5, we screened a human heart library by the yeast two-hybrid system using the full length of *CSX/NKX2-5* as a bait, and isolated a gene out of 25 positive clones, which we named *Cal*. Using the human Cal cDNA, we isolated the mouse full-length *Cal* cDNA, which encodes a protein of 375 aa (Fig. 1 A) with three tandemly arrayed LIM domains in the COOH terminus. It contains a region abundant in proline residues in the NH_2 terminus. In addition, there is a leucine-rich motif that matches the consensus sequence for NES. These salient structural features are shared among Zyxin family of LIM domain–containing proteins consisting of *Zyxin* (Beckerle, 1997), *lipoma preferred partner* (*LPP*) (Petit et al., 1996), *Ajuba* (Goyal et al., 1999), and *thyroid receptor interacting protein 6 (trip6;* Yi and Beckerle, 1998). Northern blot analysis revealed that there were two transcripts of different sizes, 3.2 and 6.0 kb, and that Cal was highly expressed in a variety of tissues (Fig. 1 B). Most abundant expression was observed in the heart and relatively abundant expression was observed in the lung, intestine, and uterus, whereas little transcript was detected in the brain and liver. RNA in situ hybridization studies revealed that *Cal* was ex-

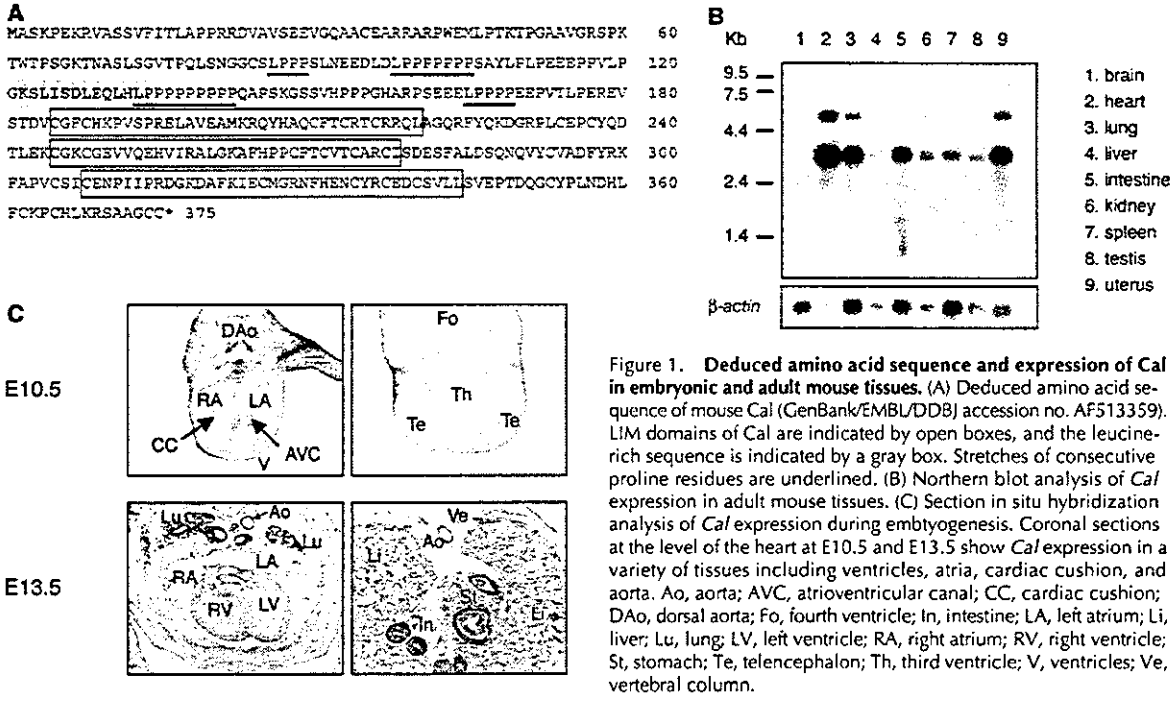

Figure 1. **Deduced amino acid sequence and expression of Cal in embryonic and adult mouse tissues.** (A) Deduced amino acid sequence of mouse Cal (GenBank/EMBL/DDBJ accession no. AF513359). LIM domains of Cal are indicated by open boxes, and the leucine-rich sequence is indicated by a gray box. Stretches of consecutive proline residues are underlined. (B) Northern blot analysis of *Cal* expression in adult mouse tissues. (C) Section in situ hybridization analysis of *Cal* expression during embtyogenesis. Coronal sections at the level of the heart at E10.5 and E13.5 show *Cal* expression in a variety of tissues including ventricles, atria, cardiac cushion, and aorta. Ao, aorta; AVC, atrioventricular canal; CC, cardiac cushion; DAo, dorsal aorta; Fo, fourth ventricle; In, intestine; LA, left atrium; Li, liver; Lu, lung; LV, left ventricle; RA, right atrium; RV, right ventricle; St, stomach; Te, telencephalon; Th, third ventricle; V, ventricles; Ve, vertebral column.

pressed in a wide variety of cell-lineages including the heart, lung, and intestine during mouse embryogenesis (Fig. 1 C). Lesser transcript was observed in the liver, and no transcript was observed in the vertebral column and encephalon.

Cal forms a complex with CSX/NKX2-5

To examine whether CSX/NKX2-5 and Cal directly interact with each other in vivo, we cotransfected COS7 cells with HA-tagged CSX/NKX2-5 and FLAG-tagged Cal. Cell lysates were subjected to immunoprecipitation using anti-FLAG antibody, and coprecipitating CSX/NKX2-5 was detected by immunoblotting with anti-HA antibody (Fig. 2 A). This result suggests that CSX/NKX2-5 and Cal associate with each other in mammalian cells as well as yeast cells.

Next, to confirm the direct interaction between CSX/NKX2-5 and Cal, and if so, to determine the domain responsible for the association, GST pull-down assays were performed with GST-Cal fusion protein and in vitro–translated CSX/NKX2-5. GST-Cal immobilized on glutathione-Sepharose beads retained in vitro–translated CSX/NKX2-5, indicating the direct interaction between CSX/NKX2-5 and Cal (Fig. 2 B). A CSX/NKX2-5 mutant lacking the homeodomain did not associate with Cal, but the homeodomain of CSX/NKX2-5 was enough for association (Fig. 2 B). These results suggest that the homeodomain of CSX/NKX2-5 is necessary and sufficient for the interaction with Cal. We also examined the binding of GST-CSX/NKX2-5 and in vitro–translated Cal and its mutants. A Cal mutant lacking all three LIM domains did not associate with CSX/NKX2-5, but Cal mutants containing at least two LIM domains did associate with CSX/NKX2-5 (Fig. 2 C). These results suggest that the LIM domains of Cal are responsible for interaction with CSX/NKX2-5.

CSX/NKX2-5 and Cal synergistically transactivate the ANP promoter

To examine the effect of Cal on transcriptional activity of CSX/NKX2-5, we performed a series of reporter assays using the luciferase reporter linked to the *ANP* promoter. When the luciferase construct containing the *ANP* promoter was cotransfected with CSX/NKX2-5 expression vector, significant fold induction of the promoter activity was observed as reported previously (Shiojima et al., 1999). Although overexpression of Cal had no effect on the *ANP* promoter, cotransfection of Cal with CSX/NKX2-5 induced much stronger transactivation than CSX/NKX2-5 alone, suggesting that CSX/NKX2-5 and Cal synergistically transactivate the *ANP* promoter (Fig. 3 A). CSX/NKX2-5 and Cal also synergistically transactivated the luciferase construct containing multimerized CSX/NKX2-5–binding sites (Fig. 3 A).

Next, we examined whether the interaction between CSX/NKX2-5 and Cal was required for the synergistic

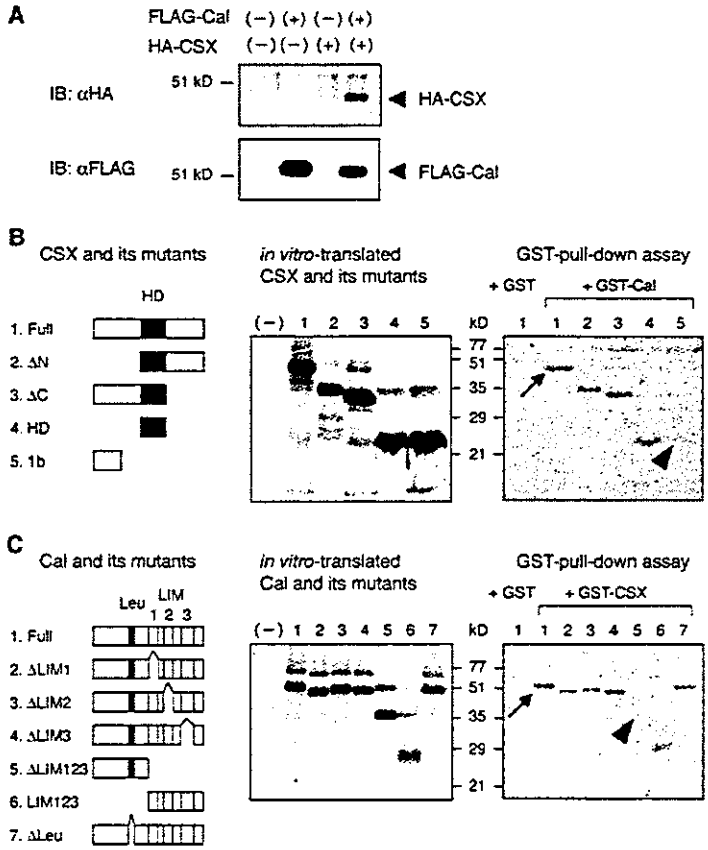

Figure 2. **Complex formation between CSX/NKX2-5 and Cal.** (A) Coimmunoprecipitation of CSX/NKX2-5 and Cal in transfected COS7 cells. Immunoprecipitates with anti-FLAG antibody were separated by SDS-PAGE and immunoblotted with anti-HA antibody (top). The same blot was reprobed with anti-FLAG antibody to confirm the presence of FLAG-tagged Cal (bottom). (B) GST pull-down assay for mapping of a region in CSX/NKX2-5 required for binding to Cal. In vitro–translated CSX/NKX2-5 and its mutants labeled with ^{35}S were incubated with GST-Cal immobilized on glutathione-Sepharose beads, and bound proteins were separated by SDS-PAGE and visualized by autoradiography. The arrow indicates the CSX/NKX2-5 protein bound to GST-Cal. A CSX/NKX2-5 mutant lacking the homeodomain did not associate with Cal (arrowhead), whereas a CSX/NKX2-5 mutant containing only the homeodomain did associate. HD, homeodomain. (C) GST pull-down assay for mapping of a region in Cal required for binding to CSX/NKX2-5. In vitro–translated Cal and its mutants labeled with ^{35}S were incubated with GST-CSX/NKX2-5. The arrow indicates the Cal protein bound to GST-CSX/NKX2-5. A Cal mutant lacking all the LIM domains did not associate with CSX/NKX2-5 (arrowhead), whereas a Cal mutant containing only the LIM domains did associate.

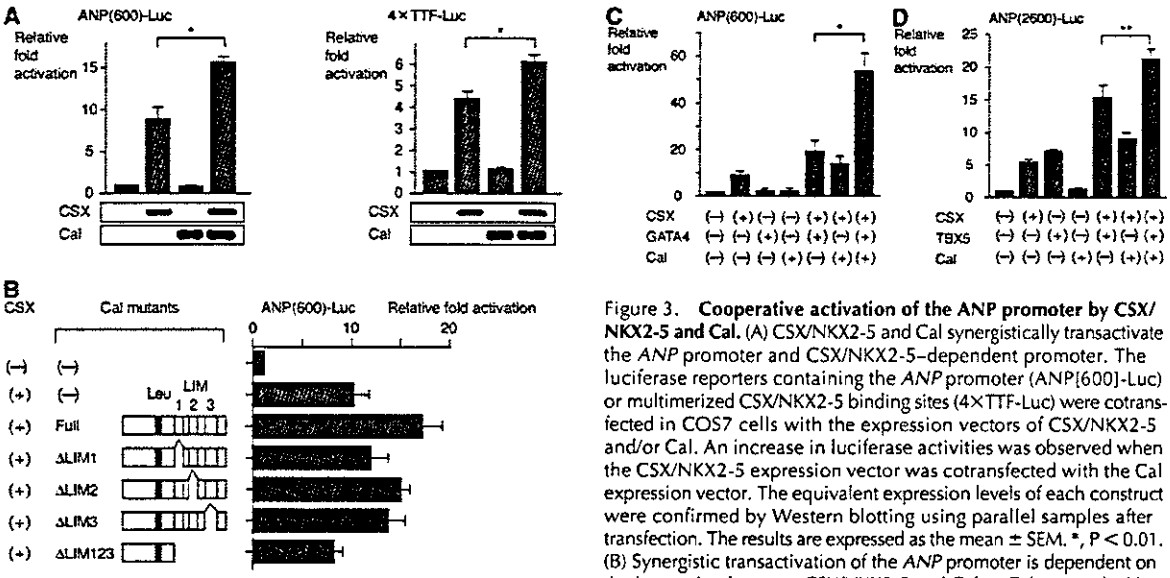

Figure 3. **Cooperative activation of the ANP promoter by CSX/NKX2-5 and Cal.** (A) CSX/NKX2-5 and Cal synergistically transactivate the *ANP* promoter and CSX/NKX2-5–dependent promoter. The luciferase reporters containing the *ANP* promoter (ANP[600]-Luc) or multimerized CSX/NKX2-5 binding sites (4×TTF-Luc) were cotransfected in COS7 cells with the expression vectors of CSX/NKX2-5 and/or Cal. An increase in luciferase activities was observed when the CSX/NKX2-5 expression vector was cotransfected with the Cal expression vector. The equivalent expression levels of each construct were confirmed by Western blotting using parallel samples after transfection. The results are expressed as the mean ± SEM. *, $P < 0.01$. (B) Synergistic transactivation of the *ANP* promoter is dependent on the interaction between CSX/NKX2-5 and Cal. A Cal mutant lacking all three LIM domains, the docking module for binding to CSX/NKX2-5, exhibited no significant cooperation on CSX/NKX2-5–induced promoter activation. The results are expressed as the mean ± SEM. (C) Cal augments synergistic transactivation between CSX/NKX2-5 and GATA-4. COS7 cells were cotransfected with the luciferase reporter containing the *ANP* promoter (ANP[600]-Luc) and the expression vectors of CSX/NKX2-5 and/or GATA-4 and/or Cal. Cotransfection with CSX/NKX2-5 and GATA-4 exhibited synergistic transactivation, that was further enhanced by additional expression of Cal. The results are expressed as the mean ± SEM. *, $P < 0.01$. (D) Cal augments synergistic transactivation between CSX/NKX2-5 and Tbx-5. Cotransfection with CSX/NKX2-5 and Tbx-5 exhibited synergistic transactivation of the *ANP* promoter (ANP[2600]-Luc), that was further augmented by additional expression of Cal. The results are expressed as the mean ± SEM. **, $P < 0.05$.

transactivation of the *ANP* promoter. Although Cal mutants lacking one LIM domain, which retain the ability to bind to CSX/NKX2-5, showed synergistic activation with CSX/NKX2-5 on the *ANP* promoter, the Cal mutant lacking the three LIM domains, which does not bind to CSX/NKX2-5, exhibited no significant cooperation on CSX/NKX2-5–induced promoter activation (Fig. 3 B). These results suggest that the synergistic transactivation was dependent on the mutual binding between CSX/NKX2-5 and Cal.

It has been reported that CSX/NKX2-5 and a zinc-finger transcription factor, GATA-4, display synergistic transcriptional activation of the *ANP* promoter (Durocher et al., 1997; Lee et al., 1998; Shiojima et al., 1999). As shown in Fig. 3 C, Cal augmented this synergistic promoter activation between CSX/NKX2-5 and GATA4. We and others reported recently that CSX/NKX2-5 and a T-box transcription factor, Tbx-5, showed synergistic transcriptional activation of the *ANP* promoter (Bruneau et al., 2001; Hiroi et al., 2001). Cal also augmented this synergistic promoter activation between CSX/NKX2-5 and Tbx-5 (Fig. 3 D).

Cal is a transactivator

To understand how Cal exhibits synergistic transcriptional activation with CSX/NKX2-5, we examined the transcriptional activity of Cal. The expression vector containing Cal fused to GAL4 DNA-binding domain was cotransfected in COS7 cells with the luciferase reporter containing the multimerized GAL4-binding sites. As shown Fig. 4, full length of Cal fused to the DNA-binding domain of GAL4 transactivated a GAL4-dependent reporter ~13.0-fold compared with DNA-binding domain of GAL4 alone. Cal mutants lacking all three LIM domains, LIM2 or LIM3 domains showed no transcriptional activity, whereas the Cal mutant containing only LIM2 and LIM3 domains showed stronger activity than the full length of Cal. Deletion of LIM1 domain showed even stronger activity, suggesting that Cal itself has the transcription-promoting activity and that its transactivation domain is localized

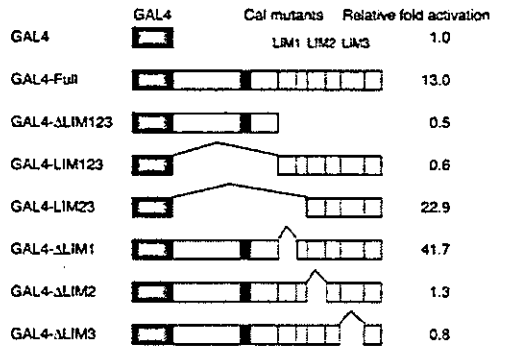

Figure 4. **Transcriptional activity of Cal.** Expression vectors encoding the GAL4 DNA binding domain fused to the indicated regions of Cal were transiently transfected into COS7 cells with the pG5luc-luciferase reporter, which contained five GAL4 binding sites. Cal fused to the DNA binding domain of GAL4 significantly transactivated a GAL4-dependent reporter, indicating that Cal possesses transcriptional activity. Cal mutants lacking LIM2 or LIM3 showed no transcriptional activity, whereas Cal mutants containing LIM2 and LIM3 showed stronger activity.